

**Last Revision March 20 2021**

**ICE, CLOUD, and Land Elevation Satellite-2  
(ICESat-2) Project**

**Algorithm Theoretical Basis Document (ATBD)**

**For**

**Land-Ice Along-Track Products Part 2:**

**Land-ice H(t)/ATL11**

**Prepared By: Benjamin Smith, Suzanne Dickinson  
Kaitlin Harbeck, Tom Neumann, David Hancock, Jeffery Lee, Benjamin Jelly**



**Goddard Space Flight Center  
Greenbelt, Maryland**

**National Aeronautics and  
Space Administration**

CHECK <https://icesatiimis.gsfc.nasa.gov>  
TO VERIFY THAT THIS IS THE CORRECT VERSION PRIOR TO USE.

30

**Abstract**

31

32

**CM Foreword**

33 This document is an Ice, Cloud, and Land Elevation Satellite-2 (ICESat-2) Project Science  
34 Office controlled document. Changes to this document require prior approval of the Science  
35 Development Team ATBD Lead or designee. Proposed changes shall be submitted in the  
36 ICESat-II Management Information System (MIS) via a Signature Controlled Request (SCoRe),  
37 along with supportive material justifying the proposed change.

38 In this document, a requirement is identified by “shall,” a good practice by “should,” permission  
39 by “may” or “can,” expectation by “will,” and descriptive material by “is.”

40 Questions or comments concerning this document should be addressed to:

41 ICESat-2 Project Science Office

42 Mail Stop 615

43 Goddard Space Flight Center

44 Greenbelt, Maryland 20771

45

46

**Preface**

47

48 This document is the Algorithm Theoretical Basis Document for the TBD processing to be  
49 implemented at the ICESat-2 Science Investigator-led Processing System (SIPS). The SIPS  
50 supports the ATLAS (Advance Topographic Laser Altimeter System) instrument on the ICESat-  
51 2 Spacecraft and encompasses the ATLAS Science Algorithm Software (ASAS) and the  
52 Scheduling and Data Management System (SDMS). The science algorithm software will produce  
53 Level 0 through Level 4 standard data products as well as the associated product quality  
54 assessments and metadata information.

55 The ICESat-2 Science Development Team, in support of the ICESat-2 Project Science Office  
56 (PSO), assumes responsibility for this document and updates it, as required, as algorithms are  
57 refined or to meet the needs of the ICESat-2 SIPS. Reviews of this document are performed  
58 when appropriate and as needed updates to this document are made. Changes to this document  
59 will be made by complete revision.

60 Changes to this document require prior approval of the Change Authority listed on the signature  
61 page. Proposed changes shall be submitted to the ICESat-2 PSO, along with supportive material  
62 justifying the proposed change.

63 Questions or comments concerning this document should be addressed to:

64 Thorsten Markus, ICESat-2 Project Scientist

65 Mail Stop 615

66 Goddard Space Flight Center

67 Greenbelt, Maryland 20771

68

**Review/Approval Page**

***Prepared by:***

Benjamin Smith  
Principal Researcher  
University of Washington  
Applied Physics Lab Polar Science Center  
1013 NE 40th Street  
Box 355640  
Seattle, WA 98105

***Reviewed by:***

*Shane Grigsby  
Postdoctoral Scholar  
Colorado School of Mines  
Department of Geophysics*

*Ellen Enderlin  
Assistant Professor  
Department of Geosciences  
Boise State University*

***Approved by:***

*Tom Neumann  
Project Scientist  
Code 615*

**\*\*\* Signatures are available on-line at: [https:// icesatiimis.gsfc.nasa.gov](https://icesatiimis.gsfc.nasa.gov) \*\*\***

**Change History Log**

Revision Level	Description of Change	SCoRe No.	Date Approved
1.0	Initial Release		
1.1	Changes for release 002. Calculate all crossovers (including near 88 S), determine the center of the y_atc search from the median of unique pair center locations.		
1.2	Changes for release 003. Add geoid and dem parameters.		

74

**List of TBDs/TBRs**

Item No.	Location	Summary	Ind./Org.	Due Date

75

76

**Table of Contents**

77 Abstract ..... ii

78 CM Foreword.....iii

79 Preface..... iv

80 Review/Approval Page ..... v

81 Change History Log ..... vi

82 List of TBDs/TBRs .....vii

83 Table of Contents.....viii

84 List of Figures ..... x

85 List of Tables ..... xi

86 1.0 INTRODUCTION ..... 1

87 2.0 BACKGROUND INFORMATION and OVERVIEW ..... 2

88 2.1 Background..... 2

89 2.2 Elevation-correction Coordinate Systems..... 3

90 2.3 Terminology: ..... 3

91 2.4 Repeat and non-repeat cycles in the ICESat-2 mission ..... 5

92 2.5 Physical Basis of Measurements / Summary of Processing..... 6

93 2.5.1 Choices of product dimensions ..... 6

94 2.6 Product coverage..... 7

95 3.0 ALGORITHM THEORY: Derivation of Land Ice H (t)/ATL11 (L3B)..... 8

96 3.1 Input data editing ..... 10

97 3.1.1 Input data editing using ATL06 parameters..... 11

98 3.1.2 Input data editing by slope..... 12

99 3.1.3 Spatial data editing ..... 13

100 3.2 Reference-Surface Shape Correction..... 13

101 3.2.1 Reference-surface shape inversion ..... 14

102 3.2.2 Misfit analysis and iterative editing ..... 15

103 3.3 Reference-shape Correction Error Estimates ..... 16

104 3.4 Calculating corrected height values for repeats with no selected pairs ..... 16

105 3.5 Calculating systematic error estimates ..... 16

106 3.6 Calculating shape-corrected heights for crossing-track data ..... 17



*ICESat-2 Algorithm Theoretical Basis Document for Land Ice H(t) (ATL11)*

*Release 003*

107 3.7 Calculating parameter averages ..... 18

108 3.8 Output data editing ..... 18

109 4.0 LAND ICE PRODUCTS: Land Ice H (t)(ATL 11/L3B) ..... 19

110 4.1.1 File naming convention..... 19

111 4.2 /ptx group..... 19

112 4.3 /ptx/ref\_surf group..... 20

113 4.4 /ptx/cycle\_stats group ..... 23

114 4.5 /ptx/crossing\_track\_data group..... 25

115 5.0 ALGORITHM IMPLEMENTATION ..... 27

116 5.1.1 Select ATL06 data for the current reference point..... 28

117 5.1.2 Select pairs for the reference-surface calculation ..... 28

118 5.1.3 Adjust the reference-point y location to include the maximum number of  
119 cycles 30

120 5.1.4 Calculate the reference surface and corrected heights for selected pairs 31

121 5.1.5 Calculate corrected heights for cycles with no selected pairs. .... 34

122 5.1.6 Calculate corrected heights for crossover data points..... 35

123 5.1.7 Provide error-averaged values for selected ATL06 parameters..... 36

124 5.1.8 Provide miscellaneous ATL06 parameters ..... 37

125 5.1.9 Characterize the reference surface ..... 38

126 6.0 Appendix A: Glossary ..... 40

127 7.0 Browse products..... 47

128 Glossary/Acronyms..... 53

129 References ..... 54

130

131 **List of Figures**

132

133 Figure Page

134 Figure 2-1. ICESat-2 repeat-track schematic..... 3

135 Figure 2-2. ATL06 data for an ATL11 reference point ..... 4

136 Figure 2-3. Potential ATL11 coverage ..... 7

137 Figure 3-1. ATL11 fitting schematic ..... 8

138 Figure 3-2. Data selection..... 10

139 Figure 5-1 Flow Chart for ATL11 Surface-shape Corrections..... 27

140 Figure 6-1. Spots and tracks, forward flight ..... 43

141 Figure 6-2. Spots and tracks, backward flight ..... 44

142 Figure 6-3. Granule regions ..... 45

143

144

**List of Tables**

145

146 Table Page

147 Table 3-1 Parameter Filters to determine the validity of segments for ATL11 estimates ..... 10

148 Table 4-1 Parameters in the */ptx/* group ..... 20

149 Table 4-2 Parameters in the */ptx/ref\_surf* group ..... 21

150 Table 4-3 Parameters in the */ptx/cycle\_stats* group ..... 23

151 Table 4-4 Parameters in the */ptx/crossing\_track\_data* group ..... 25

152

153 **1.0 INTRODUCTION**

154 This document describes the theoretical basis and implementation of the level-3b land-ice  
155 processing algorithm for ATL11, which provides time series of surface heights. The higher-level  
156 products, providing gridded height, and gridded height change will be described in supplements  
157 to this document available in early 2020.

158 ATL11 is based on the ICESat-2 ATL06 Land-ice Height product, which is described  
159 elsewhere (Smith and others, 2019a, Smith and others, 2019b). ATL06 provides height estimates  
160 for 40-meter overlapping surface segments, whose centers are spaced 20 meters along each of  
161 ICESat-2's RPTs (reference pair tracks), but displaced horizontally both relative to the RPT and  
162 relative to one another because of small (a few tens of meters or less) imprecisions in the  
163 satellite's control of the measurement locations on the ground. ATL11 provides heights  
164 corrected for these offsets between the reference tracks and the location of the ATLAS  
165 measurements. It is intended as an input for high-level products, ATL15 and ATL16, which  
166 will provide gridded estimates of ice-sheet height and height change, but also may be used alone,  
167 as a spatially-organized product that allows easy access to height-change information derived  
168 from ICESat-2.

169 ATL11 employs a technique which builds upon those previously used to measure short-term  
170 elevation changes using ICESat repeat-track data. Where surface slopes are small and the  
171 geophysical signals are large compared to background processes (i.e., ice plains and ice shelves),  
172 some studies have subtracted the mean from a collection of height measurements from the same  
173 repeat track to leave the rapidly-changing components associated with subglacial water motion  
174 (Fricker and others, 2007) or tidal flexure (Brunt and others, 2011). In regions where off-track  
175 surface slopes are not negligible, height changes can be recovered if the mean height and an  
176 estimate of the surface slope (Smith and others, 2009) are subtracted from the data, although in  
177 these regions the degree to which the surface slope estimate and the elevation-change pattern are  
178 independent is challenging to quantify.

179 ICESat-2's ATL06 product provides both surface height and surface-slope information each time  
180 it overflies its reference tracks. The resulting data are similar to that from the scanning laser  
181 altimeters that have been deployed on aircraft in Greenland and Antarctica for two decades  
182 (cite), making algorithms originally developed for these instruments appropriate for use in  
183 interpreting ATLAS data. One example is the SERAC (Surface Elevation Reconstruction and  
184 Change Detection) algorithm (Schenk & Csatho, 2012) provides an integrated framework for the  
185 derivation of elevation change from altimetry data. In SERAC, polynomial surfaces are fit to  
186 collections of altimetry data in small (< 1 km) patches, and these surfaces are used to correct the  
187 data for sub-kilometer surface topography. The residuals to the surface then give the pattern of  
188 elevation change, and polynomial fits to the residuals as a function of time give the long-term  
189 pattern of elevation change. The ATL11 algorithm is similar to SERAC, except that (1)  
190 polynomial fit correction is formulated somewhat differently, so that the ATL11 correction gives  
191 the surface height at the fit center, not the height residual, and (2) ATL11 does not include a  
192 polynomial fit with respect to time.

193

194 **2.0 BACKGROUND INFORMATION AND OVERVIEW**

195 This section provides a conceptual description of ICESat-2's ice-sheet height measurements and  
196 gives a brief description of the derived products.

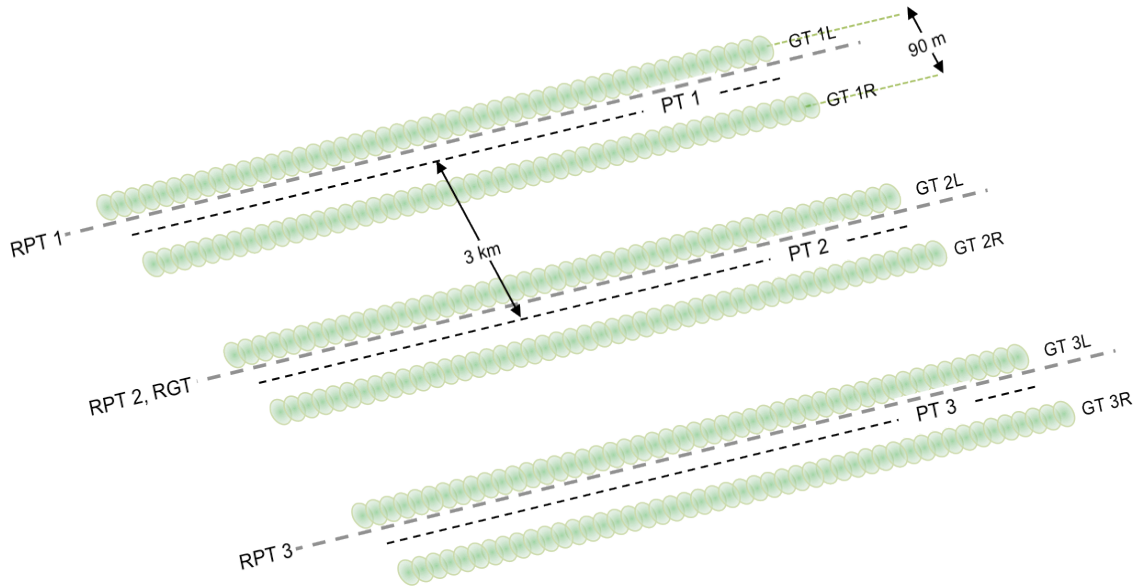
197 **2.1 Background**

198 The primary goal of the ICESat-2 mission is to estimate mass-balance rates for the Earth's ice  
199 sheets. An important step in this process is the calculation of height change at specific locations  
200 on the ice sheets. In an ideal world, a satellite altimeter would exactly measure the same point  
201 on the earth on each cycle of its orbit. However, there are limitations in a spacecraft's ability to  
202 exactly repeat the same orbit and to point to the same location. These capabilities are greatly  
203 improving with technological advances but still have limits that need to be accounted for when  
204 estimating precise elevation changes from satellite altimetry data. The first ICESat mission  
205 allowed estimates of longer-term elevation rates using along-track differencing, because  
206 ICESat's relatively precise (50-150-m) pointing accuracy, precise (4-15 m) geolocation  
207 accuracy, and small (35-70-m) footprints allowed it to resolve small-scale ice-sheet topography.  
208 However, because ICESat had a single-beam instrument, its repeat-track measurements were  
209 reliable only for measuring the mean rate of elevation change, because shorter-term height  
210 differences could be influenced by the horizontal dispersion of tracks on a sloping surface.  
211 ICESat-2 makes repeat measurements over a set of 1387 reference ground tracks (RGTs),  
212 completing a *cycle* over all of these tracks every 91 days. ICESat-2's ATLAS instrument  
213 employs a split-beam design, where each laser pulse is divided six separate beams. The beams  
214 are organized into three *beam pairs*, with each separated from its neighbors by 3.3 km (**Figure**  
215 **2-1**), each pair following a reference pair track (RPT) that is parallel to the RGT. The beams  
216 within each pair separated by 90 m, which means that each cycle's measurement over an RPT  
217 can determine the surface slope independently, and a height difference can be derived from  
218 any two measurements of an RPT. The 90-m spacing between the laser beams in each pair  
219 is equal to twice the required RMS accuracy with which ICESat-2 can be pointed at its RPTs,  
220 which means that for most, but not all, repeat measurements of a given RPT, the pairs of  
221 beams will overlap one another. To obtain a record of elevation change from the collection  
222 of paired measurements on each RPT, some correction is still necessary to account for the  
223 effects of small-scale surface topography around the RPT in the ATL06 surface heights that  
224 appear as a result of this non-exact pointing. ATL11 uses a polynomial fit to the ATL06  
225 measurements to correct for small-scale topography effects on surface heights that result  
226 from this non-exact pointing.

227 The accuracy of ICESat-2 measurements depends on the thickness of clouds between the  
228 satellite and the surface, on the reflectance, slope, and roughness of the surface, and on  
229 background noise rate which, in turn, depends on the intensity of solar illumination of the  
230 surface and the surface reflectance. It also varies from laser beam to beam, because in each  
231 of ICESat-2's beam pairs one beam (the "strong beam") has approximately four times the  
232 signal strength of the other (the "weak beam"). Parameters on the ATL06 product allow  
233 estimation of errors in each measurement, and allow filtering of most measurements with  
234 large errors due to misidentification of clouds or noise as surface returns (blunders), but to

235 enable higher precision surface change estimates, ATL11 implements further self-  
 236 consistency checks that further reduce the effects of errors and blunders.  
 237

Figure 2-1. ICESat-2 repeat-track schematic



Schematic drawing showing the pattern made by ATLAS's 6-beam configuration on the ground, for a track running from lower left to upper right. The 6 beams are grouped into 3 beam pairs with a separation between beams within a pair of 90m and a separation between beam pairs of 3.3 km. The RPTs (Reference Pair Tracks, heavily dashed lines in gray) are defined in advance of launch; the central RPT follows the RGT (Reference Ground Track, matching the nadir track of the predicted orbit). The Ground Tracks are the tracks actually measured by ATLAS (GT1L, GT1R, etc., shown by green footprints). Measured Pair Tracks (PTs, smaller dashed lines in black) are defined by the centers of the pairs of GTs, and deviate slightly from the RPTs because of inaccuracies in repeat-track pointing. The separation of GTs in each pair in this figure is greatly exaggerated relative to the separation of the PTs.

238 **2.2 Elevation-correction Coordinate Systems**

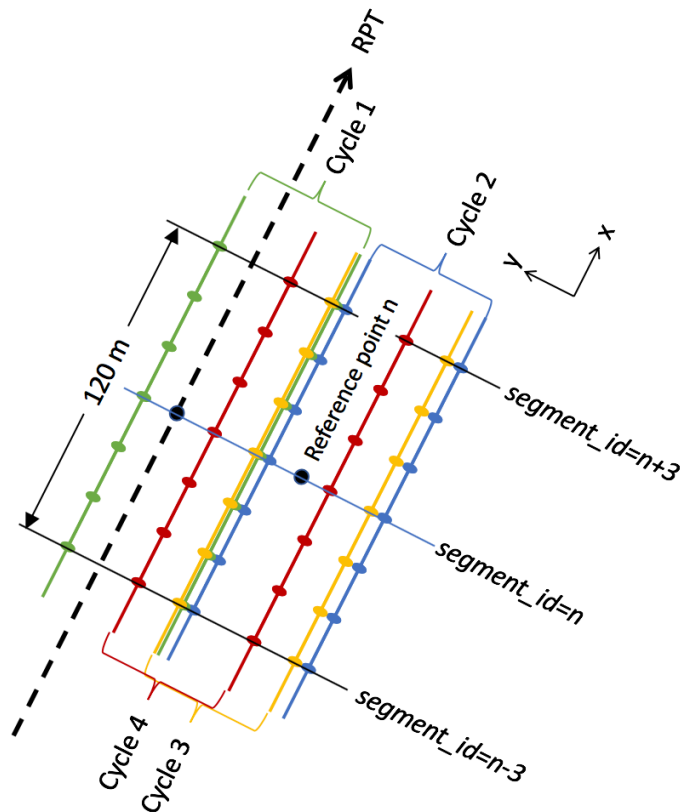
239 We perform ATL11 calculations using the along-track coordinate system described in the  
 240 ATL06 ATBD (Smith and others, 2019b, Smith and others, 2019a). The along-track coordinate  
 241 is measured parallel to the RGT, starting at each RGT's origin at the equator. The across-track  
 242 coordinate is measured to the left of the RGT, so that the two horizontal basis vectors and the  
 243 local vertical vector form a right-handed coordinate system.

244 **2.3 Terminology:**

245 Some of the terms that we will use in describing the ATL11 fitting process and the data  
 246 contributing are:

247 *RPT*: Reference pair track  
248 *Cycle*: ICESat-2 has 1387 distinct reference ground tracks, which its orbit covers every 91 days.  
249 One repeat measurement of these reference ground tracks constitutes a cycle.  
250 *ATL06 segment*: A 40-meter segment fit to a collection of ATL03 photon-event data, as  
251 described in the ATL06 ATBD  
252 *ATL06 pair*: Two ATL06 segments from the same cycle with the same *segment\_id*. By  
253 construction, both segments in the ATL06 pair have the same along-track coordinate, and are  
254 separated by the beam-to-beam spacing (approximately 90 m) in the across-track direction  
255 *ATL11 RPT point*: The expected location of each ATL11 point on the RPT, equivalent to the  
256 beginning of every third geosegment on the RPT, or the center of every third ATL06 segment.  
257 *ATL11 reference point*: an *ATL11 RPT point* shifted in the across-track direction to better match  
258 the geometry of the available ATL06 data.  
259 *ATL11 fit*: The data and parameters associated with a single ATL11 reference point. This  
260 includes corrected heights from all available cycles  
261  
262 ATL11 calculates elevations and elevation differences based on collections of segments from the  
263 same beam pair but from different cycles. ATL11 is posted every 60 m, which corresponds to  
264 every third ATL06 *segment\_id*, and includes ATL06 segments spanning three segments before  
265 and after the central segment, so that the ATL11 uses data that span 120 m in the along-track  
266 direction. ATL11 data are centered on *reference points*, which has the same along-track  
267 coordinate as its central ATL06 segment, but is displaced in the across-track direction to better  
268 match the locations of the ATL06 measurements from all of the cycles present (see section  
269 3.1.3).

Figure 2-2. ATL06 data for an ATL11 reference point



Schematic of ATL06 data for an ATL11 reference point centered on segment  $n$ , based on data from four cycles. The segment centers span 120 m in the along-track data, and the cycles are randomly displaced from the RPT in the across-track direction. The reference point has an along-track location that matches that of segment  $n$ , and an across-track position chosen to match the displacements of the cycles.

270

271 **2.4 Repeat and non-repeat cycles in the ICESat-2 mission**

272 In the early part of the ICESat-2 mission, an error in the configuration of the start trackers  
 273 prevented the instrument from pointing precisely at the RGTs. As a result, all data from cycles 1  
 274 and 2 were measured between one and two kilometers away from the RGTs, with offsets that  
 275 varied in time and as a function of latitude. The measurements from cycles 1 and 2 still give  
 276 high-precision measurements of surface height, but repeat-track measurements from ICESat-2  
 277 begin during cycle 3, in April of 2019. ATL11 files will be generated for ATL06 granules from  
 278 cycles 1 and 2, but these will contain only one cycle of data, plus crossovers, because the  
 279 measurements from these cycles (which are displaced from the RPTs by several kilometers) will  
 280 not be repeated. We expect the measurements from cycles 1 and 2 to be useful as a reduced-  
 281 resolution (compared to ATL06) mapping of the ice sheet, which may prove useful in DEM  
 282 generation and in comparisons with other altimetry missions. For cycles 3 and after, each  
 283 ATL11 granule will contain all available cycles for each RGT (i.e. from cycle 3 onwards), and  
 284 will contain crossovers between the repeat cycles and cycles 1 and 2.



285 Outside the polar regions, ICESat-2 is pointed to minimize gaps between repeat measurements,  
286 and so does not make repeat measurements over its ground tracks. ATL11 is only calculated  
287 within the repeat-pointing mask (see Figure ???), which covers areas poleward of 60°N and  
288 60°S.  
289

## 290 **2.5 Physical Basis of Measurements / Summary of Processing**

291 Surface slopes on the Antarctic and Greenland ice sheets are generally small, with magnitudes  
292 less than two degrees over 99% of Antarctica’s area. Smaller-scale (0.5-3 km) undulations,  
293 generated by ice flow over hilly or mountainous terrain may have amplitudes of up to a few  
294 degrees. Although we expect that the surface height will change over time, slopes and locations  
295 of these smaller-scale undulation are likely controlled by underlying topography and should  
296 remain essentially constant over periods of time comparable with the expected 3-7 duration of  
297 the ICESat-2 mission. This allows us to use estimates of ice-sheet surface shape derived from  
298 data spanning the full mission to correct for small (<130-m) differences in measurement  
299 locations between repeat measurements of the same RPT, to produce records of height change  
300 for specific locations. To account for changes in the ice-sheet surface slope associated with  
301 gradients in thinning, we also solve for the rate of surface-slope change, when sufficient data are  
302 available. Further, we can use the surface slope estimates in ATL06 to determine whether  
303 different sets of measurements for the same fit center are self-consistent: We can assume that if  
304 an ATL06 segment shows a slope significantly different from others measured near the same  
305 reference point it likely is in error. The combination of parameters from ATL06 and these self-  
306 consistency checks allows us to generate time series based on the highest-quality measurements  
307 for each reference point, and our reference surface calculation lets us correct for small-scale  
308 topography and to estimate error magnitudes in the corrected data.

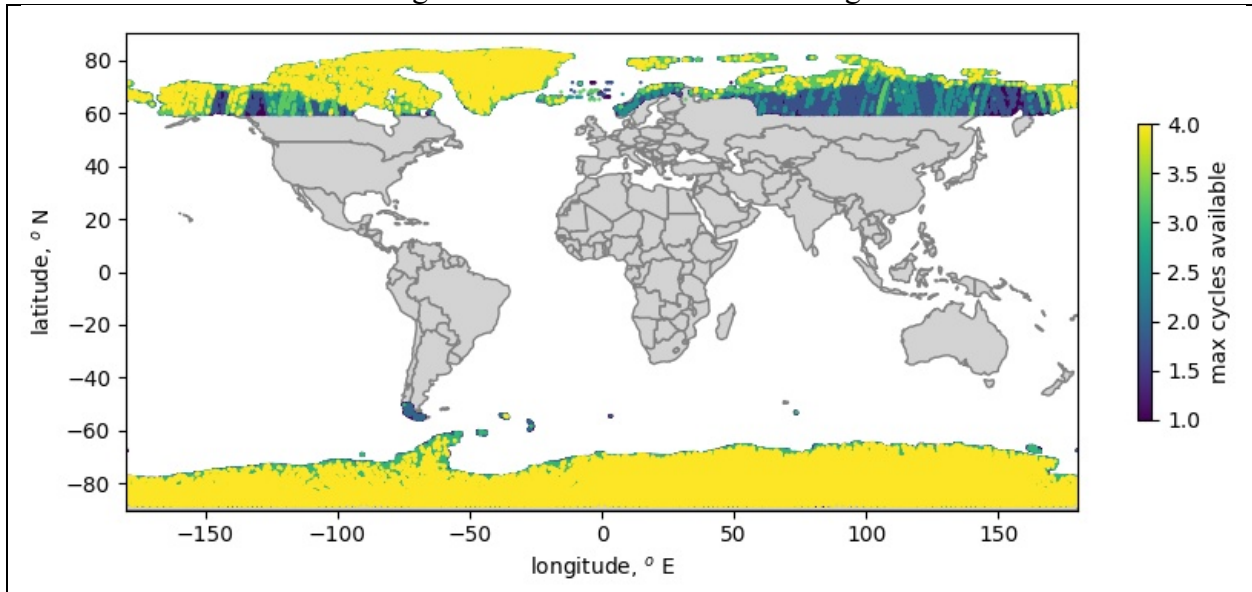
### 309 **2.5.1 Choices of product dimensions**

310 We have chosen a set of dimensions for the ATL11 fitting process with the goal of creating a  
311 product that is conveniently sized for analysis of elevation changes, while still capturing the  
312 details of elevation change in outlet glaciers. The assumption that ice-sheet surface can be  
313 approximated by a low-degree polynomial becomes untenable as data from larger and larger  
314 areas are included in the calculation; therefore we use data from the smallest feasible area to  
315 define our reference surface, while still including enough data to reduce the sampling error in the  
316 data and to allow for the possibility that at least one or two will encounter a flat surface, which  
317 greatly improves the chances that each cycle will be able to measure surface comparable to one  
318 another. Each ATL11 point uses data from an area up to 120 m in the along-track direction by  
319 up to 130 m in the across-track direction. We have chosen the cross-track search distance  
320 ( $L_{\text{search\_XT}}$ ) to be 65 m, approximately equal to half the beam spacing, plus three times the  
321 observed 6.5 m standard deviation of the across-track pointing accuracy for cycles 3 and 4 in  
322 Antarctica. We chose the across-track search distance ( $L_{\text{search\_AT}}$ ) to be 60 m, approximately  
323 equal to  $L_{\text{search\_XT}}$ , so that the full  $L_{\text{search\_AT}}$  search window spans three ATL06 segments before  
324 and after the central segment for each reference point. The resulting along-track resolution is

325 around one third that of ATL06, but still allows 6-7 distinct elevation-change samples across a  
 326 small (1-km) outlet glacier.

327 **2.6 Product coverage**

Figure 2-3. Potential ATL11 coverage



Maximum number of valid repeat measurements from an ATL11 file for each 10-km segment of pair track 2. Yellower colors indicate areas where ICESat-2 has systematically pointed at the RGTs.

328 Over the vegetated parts of the Earth, ICESat-2 makes spatially dense measurements, measuring  
 329 tracks parallel to the reference tracks in a strategy that will eventually measure global vegetation  
 330 with a track-to-track spacing better than 1 km. Because ATL11 relies upon repeat measurements  
 331 over reference tracks to allow the calculation of its reference surfaces, ATL11 is generated for  
 332 ICESat-2 subregions 3-5 and 10-12 (global coverage, north and south of 60 degrees). Repeat  
 333 measurements are limited to Antarctica, Greenland, and the High Arctic islands (Figure 2-3),  
 334 although in other areas the fill-in strategy developed for vegetation measurements allows some  
 335 repeat measurements. In regions where ICESat-2 was not pointed to the repeat track, most  
 336 ATL11 reference points will provide one measurement close to the RPT. Crossover data are  
 337 available for many of these points, though their distribution in time is not regular. A future  
 338 update to the product may provide crossover measurements for lower-latitude areas, but the  
 339 current product format is not designed to allow this.

340 **3.0 ALGORITHM THEORY: DERIVATION OF LAND ICE H (T)/ATL11 (L3B)**

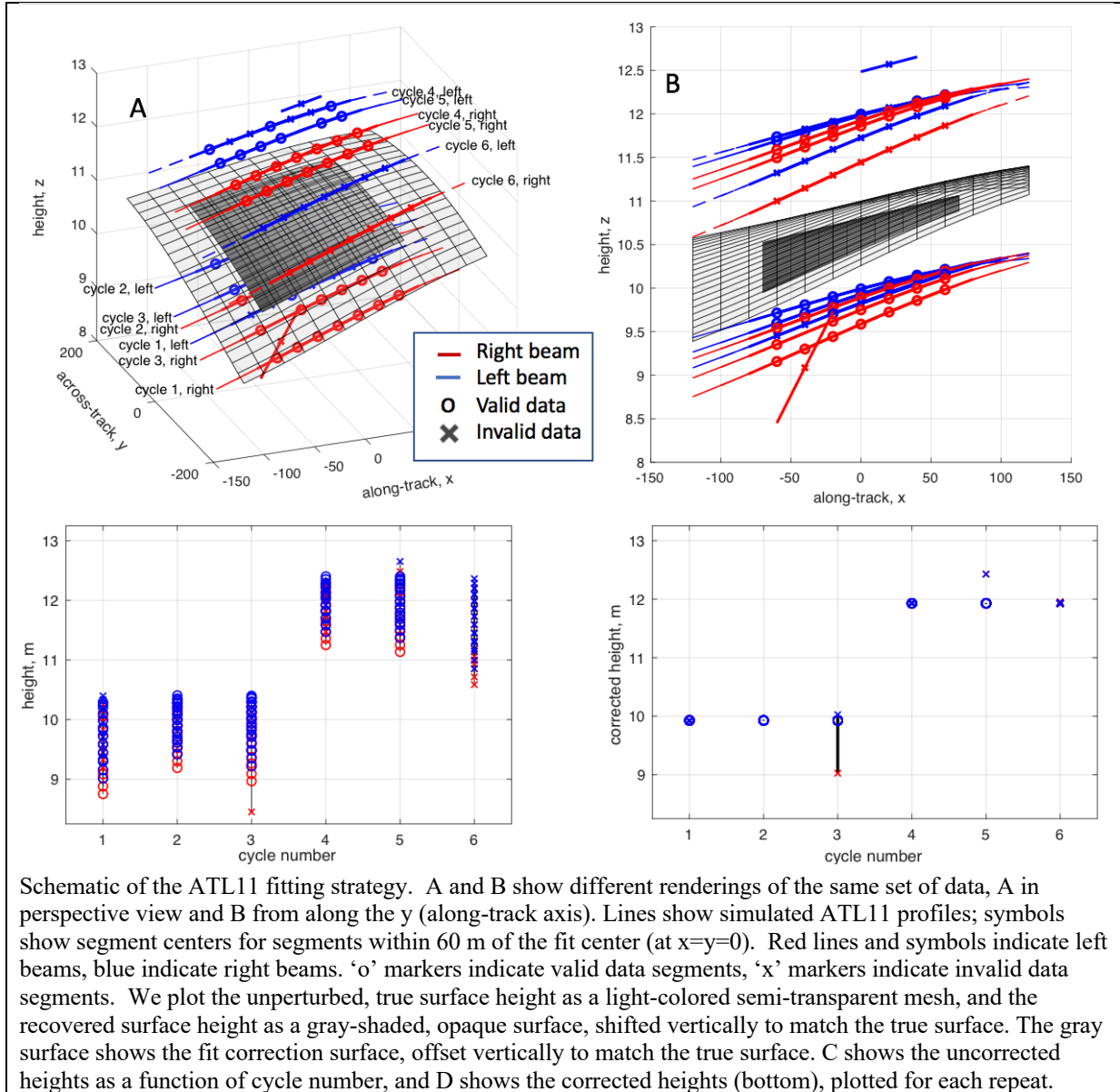
341 In this section, we describe in detail the algorithms used in calculating the ATL11 land-ice  
342 parameters. This product is intended to provide time series of surface heights for land-ice and  
343 ice-shelf locations where ICESat-2 operates in repeat-track mode (*i.e.* for polar ice), along with  
344 parameters useful in determining whether each height estimate is valid or a result of a variety of  
345 potential errors (see ATL06 ATBD, section 1).

346 ATL11 height estimates are generated by correcting ATL06 height measurements for the  
347 combined effects of short-scale (40-120-m) surface topography around the fit centers and small  
348 (up to 130-m) horizontal offsets between repeat measurements. We fit a polynomial reference  
349 surface to height measurements from different cycles as a function of horizontal coordinates  
350 around the fit centers, and use this polynomial surface to correct the height measurements to the  
351 fit center. The resulting values reflect the time history of surface heights at the reference points,  
352 with minimal contributions from small-scale local topography.

353 In this algorithm, for a set of reference points spaced every 60 meters along each RPT (centered  
354 on every third segment center), we consider all ATL06 segments with centers within 60 m along-  
355 track and 65 m across-track of the reference point, so that each ATL11 fit contains as many as  
356 seven distinct along-track segments from each laser beam and cycle. We select a subset of these  
357 segments with consistent ATL06 slope estimates and small error estimates, and use these  
358 segments to define a time-variable surface height and a polynomial surface-shape model. We  
359 then use the surface-shape model to calculate corrected heights for the segments from cycles not  
360 included in the initial subset. We propagate errors for each of these steps to give formal errors  
361 estimates that take into account the sampling error from ATL06, and propagate the geolocation  
362 errors with the slope of the surface-shape model to give an estimate of systematic errors in the  
363 height estimates.

---

Figure 3-1. ATL11 fitting schematic



Schematic of the ATL11 fitting strategy. A and B show different renderings of the same set of data, A in perspective view and B from along the y (along-track axis). Lines show simulated ATL11 profiles; symbols show segment centers for segments within 60 m of the fit center (at  $x=y=0$ ). Red lines and symbols indicate left beams, blue indicate right beams. ‘o’ markers indicate valid data segments, ‘x’ markers indicate invalid data segments. We plot the unperturbed, true surface height as a light-colored semi-transparent mesh, and the recovered surface height as a gray-shaded, opaque surface, shifted vertically to match the true surface. The gray surface shows the fit correction surface, offset vertically to match the true surface. C shows the uncorrected heights as a function of cycle number, and D shows the corrected heights (bottom), plotted for each repeat.

364  
365  
366  
367  
368  
369  
370  
371  
372  
373  
374  
375

Figure 3-1 shows a schematic diagram of the fitting process. In this example, we show simulated ATL06 height measurements for six 91-day orbital cycles over a smooth ice-sheet surface (transparent grid). Between cycles 3 and 4, the surface height has risen by 2 m. Two of the segments contain errors: The weak beam for one segment from repeat 3 is displaced downward and has an abnormal apparent slope in the  $x$  direction, and one segment from repeat 5 is displaced upwards, so that its pair has an abnormal apparent slope in the  $y$  direction. Segments falling within the across and along-track windows of the reference point (at  $x=y=0$  in this plot) are selected, and fit with a polynomial reference surface (shown in gray). When plotted as a function of cycle number (panel C), the measured heights show considerable scatter but when corrected to the reference surface (panel D), each cycle shows a consistent height, and the segments with errors are clearly distinct from the accurate measurements.

376 **3.1 Input data editing**

377 Each ATL06 measurement includes location estimates, along- and across-track slope estimates,  
 378 and PE (Photon-Event)-height misfit estimates. To calculate the reference surface using the most  
 379 reliable subset of available data, we perform tests on the surface-slope estimates and error  
 380 statistics from each ATL06-pair to select a self-consistent set of data. These tests determine  
 381 whether each pair of measurements is *valid* and can be used in the reference-shape calculation or  
 382 is *invalid*. Segments from invalid pairs may be used in elevation-change calculations, but not in  
 383 the reference-shape calculation.

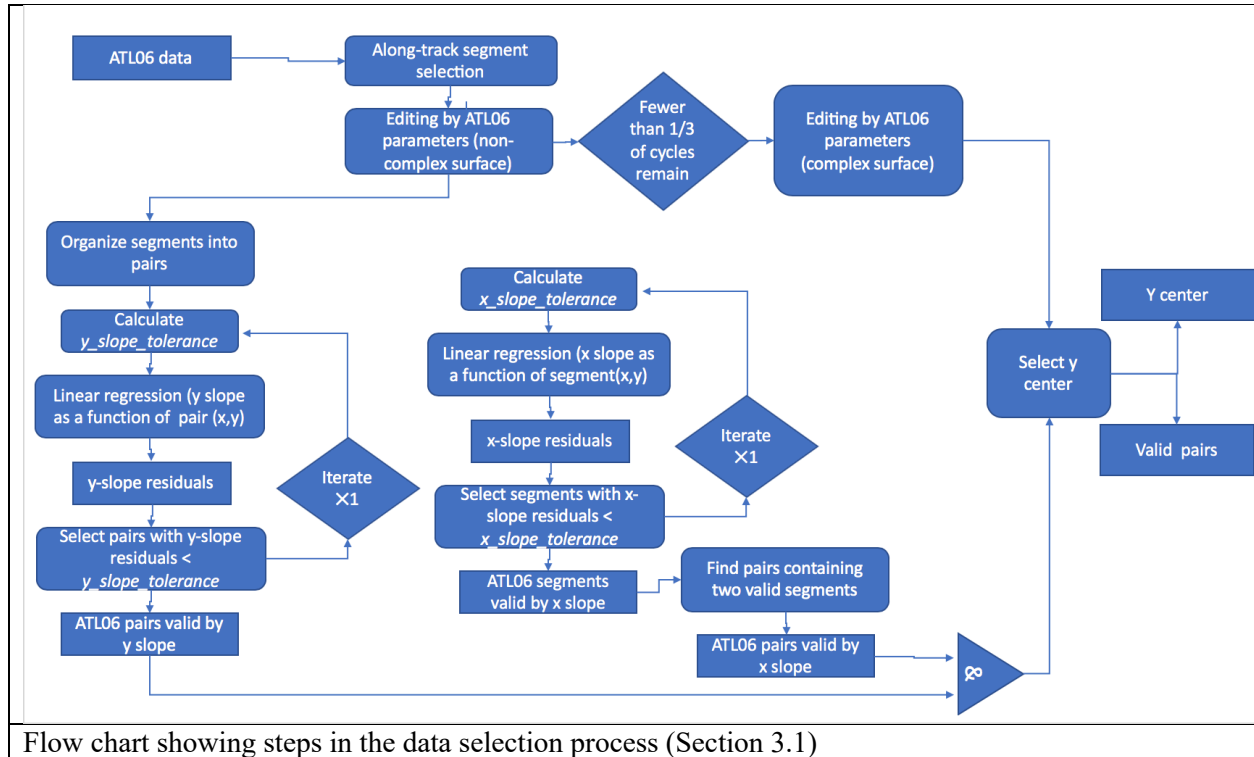
384 A complete flow chart of the data-selection process is shown in Figure 3-2, and the parameters  
 385 used to make these selections and their values are listed in Table 3-1.

386

387 **Table 3-1 Parameter Filters to determine the validity of segments for ATL11 estimates**

<b>complex_surface _flag</b>	<b>Segment parameter</b>	<b>Filter strategy</b>	<b>Section</b>
0	<i>ATL06_quality_summary</i>	<i>ATL06_quality_summary</i> =0 (indicates high-quality segments)	3.1.1
1	<i>SNR_significance</i>	<i>SNR_significance</i> < 0.02 (indicates low probability of surface-detection blunders)	3.1.1
0 or 1	Along-track differences	Minimum height difference between the endpoints of a segment and the middles of its neighbors must be < 2 m (for smooth surfaces) or < 10 m (for complex surfaces)	3.1.1
0 or 1	<i>h_li_sigma</i>	<i>h_li_sigma</i> < max(0.05, 3*median( <i>h_li_sigma</i> ))	3.1.1
0 or 1	Along-track slope	<i>r_slope_x</i>   < 3 <i>slope_tolerance_x</i>	3.1.2
0 or 1	Across-track slope	<i>r_slope_y</i>   < 3 <i>slope_tolerance_y</i>	3.1.2
0 or 1	Segment location	<i>x_atc-x0</i>   < <i>L_search_XT</i>   <i>y_atc-y0</i>   < <i>L_search_AT</i>	3.1.3

Figure 3-2. Data selection



Flow chart showing steps in the data selection process (Section 3.1)

388

### 3.1.1 Input data editing using ATL06 parameters

390 For each reference point, we collect all ATL06 data from all available repeat cycles that have  
 391 *segment\_id* values within  $\pm 3$  of the reference point (inclusive) and that are on the same *rgt* and  
 392 pair track as the reference point. The *segment\_id* criterion ensures that the segment centers are  
 393 within  $\pm 60$  m of the reference point in the along-track direction. We next check that the ATL06  
 394 data are close to the pre-defined reference track, by rejecting all ATL06 segments that are more  
 395 than 500 m away from the nominal pair across-track coordinates (-3200, 0, and 3200 meters for  
 396 right, center, and left pairs, respectively). This removes data that were intentionally or  
 397 accidentally collected with ATLAS pointed off nadir (i.e. for calibration scan maneuvers).  
 398 ATL06 contains some segments with signal-finding blunders (Smith et al., 2019). To avoid  
 399 having these erroneous segments contaminate ATL11, we filter using one of two sets of tests,  
 400 depending on surface roughness. We identify high-quality ATL06 segments, using parameters  
 401 that depend on whether the surface is identified as smooth or rough, as follows:  
 402 1) For smooth ice-sheet surfaces, we use the ATL06 *ATL06\_quality\_summary* parameter,  
 403 combined with a measure of along-track elevation consistency, *at\_min\_dh*, that is calculated as  
 404 part of ATL11. *ATL06\_quality\_summary* is based on the spread of the residuals for each  
 405 segment, the along-track surface slope, the estimated error, and the signal strength. Zero values  
 406 indicate that no error has been found. We define the along-track consistency parameter  
 407 *at\_min\_dh* as the minimum absolute difference between the heights of the endpoints of each  
 408 segment and the center heights of the previous and subsequent segments. Its value will be small  
 409 if a segment's height and slope are consistent with at least one of its neighbors. For smooth

410 surfaces, we require that the *at\_min\_dh* values be less than 2 m. Over smooth ice-sheet surfaces,  
 411 the 2-m threshold eliminates most blunders without eliminating a substantial number of high-  
 412 quality data points.

413 2) For rough, crevassed surfaces, the smooth-ice strategy may not identify a sufficient number of  
 414 pairs for ATL11 processing to continue. If fewer than one third of the original cycles remain  
 415 after the smooth-surface criteria are applied, we relax our criteria, using the signal-to-noise ratio  
 416 (based on the ATL06 *segment\_stats/snr\_significance* parameter) to select the pairs to include in  
 417 the fit, and require that the *at\_min\_dh* values be less than 10 m. If we relax the criteria in this  
 418 way, we mark the reference point as having a complex surface using the  
 419 *ref\_surf/complex\_surface\_flag*, which limits the degree of the polynomial used in the reference  
 420 surface fitting to 0 or 1 in each direction.

421 For either smooth or rough surfaces, we perform an additional check using the magnitude of  
 422 *h\_li\_sigma* for each segment. If any segment's value is larger than three times the maximum of  
 423 0.05 m and the median *h\_li\_sigma* for the valid segments for the current reference point, it is  
 424 marked as invalid. The limiting 0.05 m value prevents this test from removing high-quality data  
 425 over smooth ice-sheet surfaces, where errors are usually small.

426 Each of these tests applies to values associated with ATL06 segments. When the tests are  
 427 complete, we check each ATL06 pair (*i.e.* two segments for the same along-track location from  
 428 the same cycle) and if either of its two segments has been marked as invalid, the entire pair is  
 429 marked as invalid.

### 430 3.1.2 Input data editing by slope

431 The segments selected in 3.1.1 may include some high-quality segments and some lower-quality  
 432 segments that were not successfully eliminated by the data-editing criteria. We expect that the  
 433 ATL06 slope fields (*dh\_fit\_dx*, and *dh\_fit\_dy*) for the higher-quality data should reflect the  
 434 shape of an ice-sheet surface with a spatially consistent surface slope around each reference  
 435 point, but that at least some of lower-quality data should have slope fields that outliers relative to  
 436 this consistent surface slope. In this step, we assume that the slope may vary linearly in *x* and *y*,  
 437 and so use residuals between the slope values and a regression of the slope values against *x* and *y*  
 438 to identify the data with inconsistent slope values. The data with large residuals are marked as  
 439 *invalid*.

440 Starting with valid pairs from 3.2.1, we first perform a linear regression between the *y* slopes of  
 441 the pairs and the pair-center *x* and *y* positions. The residuals to this regression define one  
 442 *y\_slope\_residual* for each pair. We compare these residuals against a *y\_slope\_tolerance*:

$$y\_slope\_tolerance = \max(0.01, 3 \text{ median } (dh\_fit\_dy\_sigma), 3 RDE \quad 1 \\ (y\_slope\_residuals))$$

443 Here RDE is the Robust Difference Estimator, equal to half the difference between the 16<sup>th</sup> and  
 444 84<sup>th</sup> percentiles of a distribution, and the minimum value of 0.01 ensures that this test does not  
 445 remove high-quality segments in regions where the residuals are very consistent. If any pairs  
 446 have a *y\_slope\_residual* greater than *y\_slope\_tolerance*, we remove them from the group of valid  
 447 pairs, then repeat the regression, recalculate *y\_slope\_tolerance*, and retest the remaining pairs.  
 448 We then return to the pairs marked as *valid* from 3.1.1, and perform a linear regression between  
 449 the *x* slopes of the segments within the pairs and the segment-center *x* and *y* positions. The

450 residuals to this regression define one  $x\_slope\_residual$  for each segment. We compare these  
 451 residuals against an  $x\_slope\_tolerance$ , calculated in the same way as (1), except using segment  $x$   
 452 slopes and residuals instead of pair  $y$  slopes. As with the  $y$  regression, we repeat this procedure  
 453 once if any segments are eliminated in the first round.  
 454 After both the  $x$  and  $y$  regression procedures are complete, each pair of segments is marked as  
 455 *valid* if both of its  $x$  residuals are smaller than  $slope\_tolerance\_x$  and its  $y$  residual is smaller than  
 456  $slope\_tolerance\_y$ .

### 457 3.1.3 Spatial data editing

458 The data included in the reference-surface fit fall in a “window” defined by a  $2L_{search\ XT}$  by  
 459  $2L_{search\ AT}$  rectangle, centered on each reference point. Because the across-track location of the  
 460 repeat measurements for each reference point are determined by the errors in the repeat track  
 461 pointing of ATLAS, a data selection window centered on the RPT in the  $y$  direction will not  
 462 necessarily capture all of the available cycles of data. To improve the overlap between the  
 463 window and the data, we shift the reference point in the  $y$  direction so that the window includes  
 464 as many valid beam pairs as possible. We make this selection after the parameter-based (3.1.1)  
 465 and slope-based (3.1.2) editing steps because we want to maximize the number high-quality pairs  
 466 included, without letting the locations of low-quality segments influence our choice of the  
 467 reference-point shift.

468 We select the across-track offset for each reference point by searching a range of offset values,  $\delta$ ,  
 469 around the RPT to maximize the following metric:

$$M(\delta) = \frac{[number\ of\ unique\ valid\ pairs\ entirely\ contained\ in\ \delta \pm L_{search\ XT}] + [number\ of\ unpaired\ segments\ contained\ in\ \delta \pm L_{search\ XT}]/100}{2}$$

470 Maximizing this metric allows the maximum number of pairs with two valid segments to be  
 471 included in the fit, while also maximizing the number of segments included close to the center of  
 472 the fit. If multiple values of  $\delta$  have the same  $M$  value we choose the median of those  $\delta$  values.

473 The across-track coordinate of the adjusted reference point is then  $y_0 + \delta_{max}$ , where  $y_0$  is the  
 474 across-track coordinate of the unperturbed reference point. After this adjustment, the segments  
 475 in pairs that are contained entirely in the across-track interval  $\delta \pm L_{search\ XT}$  are identified as  
 476 *valid* based on the spatial search.

477 The location of the adjusted reference point is reported in the data group for each pair track, with  
 478 corresponding local coordinates in the *ref\_surf* subgroup: */ptx/ref\_surf/x\_atc*, */ptx/ref\_surf/y\_atc*.

## 480 3.2 Reference-Surface Shape Correction

481 To calculate the reference-surface shape correction, we construct the background surface shape  
 482 from valid segments selected during 3.1 and 3.2, using a least-squares inversion that separates  
 483 surface-shape information from elevation-change information. This produces surface shape-  
 484 corrected height estimates for cycles containing at least one valid pair, and a surface-shape  
 485 model that we use in later steps (3.4, 3.6) to calculate corrected heights for cycles that contain no  
 486 valid pairs and to calculate corrected heights for crossing tracks.



487 **3.2.1 Reference-surface shape inversion**

488 The reference-shape inversion solves for a reference surface and a set of corrected-height values  
 489 that represent the time-varying surface height at the reference point. The inversion involves  
 490 three matrices:

491 (i): a polynomial surface shape matrix, **S**, that describes the functional basis for the spatial part of  
 492 the inversion:

$$\mathbf{S} = \left[ \left( \frac{x - x_0}{l_0} \right)^p \left( \frac{y - y_0}{l_0} \right)^q \right] \quad 3$$

493 Here  $x_0$  and  $y_0$  are equal to the along-track coordinates of the adjusted reference point,  
 494 */ptx/ref\_surf/x\_atc* and */ptx/ref\_surf/y\_atc*, respectively. **S** has one column for each permutation  
 495 of  $p$  and  $q$  between zero and the degree of the surface polynomial in each dimension, but does  
 496 not include a  $p=q=0$  term. The degree is chosen to be no more than 3 (in the along-track  
 497 direction) or 2 (in the across-track direction), and to be no more than the number of distinct pair-  
 498 center  $y$  values (in the across-track direction) or more than 1 less than the number of distinct  $x$   
 499 values (in the along-track direction) in any cycle, with distinct values defined at a resolution of  
 500 20 m in each direction. The scaling factor,  $l_0$ , ensures that the components of **S** are on the order  
 501 of 1, which improves the numerical accuracy of the computation. We set  $l_0=100$  m, to  
 502 approximately match the intra-pair beam spacing.

503 (ii): a matrix that encodes the repeat structure of the data, that accounts for the height-change  
 504 component of the inversion:

$$\mathbf{D} = [\delta(i, 1), \delta(i, 2), \dots, \delta(i, N)] \quad 4$$

505 Here  $\delta$  is the delta function, equal to 1 when its arguments are equal, zero otherwise, and  $i$  is an  
 506 index that increments by one for each distinct cycle in the selected data.

507 (iii): a matrix that describes the linear rate of change in the surface slope over the course of the  
 508 mission:

$$\mathbf{S}_t = \left[ \left( \frac{x - x_0}{l_0} \right) \left( \frac{t - t_0}{\tau} \right), \left( \frac{y - y_0}{l_0} \right) \left( \frac{t - t_0}{\tau} \right) \right] \quad 5$$

509 Here  $t_0$  is equal to *slope\_change\_t0*, the mid-point of the mission at the time that ATL11 is  
 510 generated, halfway between start repeat track pointing (the beginning of cycle 3) and either the  
 511 end of the mission or the processing time (*slope\_change\_t0* is an attribute of each ATL11  
 512 file). This implies that on average,  $(t - t_0)$  will have a zero mean. The time-scaling factor,  $\tau$ , is  
 513 equal to one year (86400\*365.25 seconds). This component will only be included in ATL11  
 514 once eight complete cycles of data are available on the RGTs (after cycle 10 of the mission).  
 515 The surface shape, slope change, and height time series are estimated by forming a composite  
 516 design matrix, **G**, where

$$\mathbf{G} = [\mathbf{S} \ \mathbf{S}_t \ \mathbf{D}], \quad 6$$

517 and a covariance matrix, **C**, containing the squares of the segment-height error estimates on its  
 518 diagonal. The surface-shape polynomial and the height changes are found:

$$\begin{aligned} [\mathbf{s}, \mathbf{s}_t, \mathbf{z}_c] &= \mathbf{G}^{-\mathbf{g}} \mathbf{z} \\ \text{where} & \\ \mathbf{G}^{-\mathbf{g}} &= [\mathbf{G}^T \mathbf{C}^{-1} \mathbf{G}]^{-1} \mathbf{G}^T \mathbf{C}^{-1} \end{aligned} \quad 7$$

519 The notation  $[\ ]^{-1}$  designates the inverse of the quantity in brackets, and  $\mathbf{z}$  is the vector of segment  
 520 heights. The parameters derived in this fit are  $\mathbf{s}$ , a vector of surface-shape polynomial  
 521 coefficients,  $\mathbf{s}_t$ , the mean rate of surface-slope change, and  $\mathbf{z}_c$ , a vector of corrected height values,  
 522 giving the height at  $(lat_0, lon_0)$  as inferred from the height measurements and the surface  
 523 polynomial. The matrix  $\mathbf{G}^g$  is the generalized inverse of  $\mathbf{G}$ . The values of  $\mathbf{s}$  are reported in the  
 524 *ref\_surf/poly\_ref\_surf* parameter, as they are calculated from (6), with no correction made for the  
 525 scaling in (3). The values for the slope-change rates are reported in *ref\_surf/slope\_change\_rate*,  
 526 after rescaling to units of *years<sup>-1</sup>*.

### 527 3.2.2 Misfit analysis and iterative editing

528 If blunders remain in the data input to the reference-surface calculation, they can lead to  
 529 inaccurate reference surfaces. To help remove these blunders, we iterate the inversion procedure  
 530 in 3.2.1, eliminating outlying data points based on their residuals to the reference surface.

531 To determine whether outliers may be present, we calculate the chi-squared misfit between the  
 532 data and the fit surface based on the data covariance matrix and the residual vector,  $r$ :

$$\chi^2 = r^T \mathbf{C}^{-1} r \quad 8$$

533 To determine whether this misfit statistic indicates consistency between the polynomial surface  
 534 and the data we use a P statistic, which gives the probability that the given  $\chi$  value would be  
 535 obtained from a random Gaussian distribution of data points with a covariance matrix  $\mathbf{C}$ . If the  
 536 probability is less than 0.025, we perform some further filtering/editing: we calculate the RDE of  
 537 the scaled residuals, eliminate any pairs containing a segment whose scaled residual magnitude is  
 538 larger than three times that value, and repeat the remaining segments.

539 After each iteration, any column of  $\mathbf{G}$  that has a uniform value (i.e. all the values are the same) is  
 540 eliminated from the calculation, and the corresponding value of the left-hand side of equation 7  
 541 is set to zero. Likewise, if the inverse problem has become less than overdetermined (i.e., the  
 542 number of data is smaller than the number of unknown values they are constraining), the  
 543 polynomial columns of  $\mathbf{G}$  are eliminated one by one until the number of data is greater than the  
 544 number of unknowns. Columns are eliminated in descending order of the sum of  $x$  and  $y$   
 545 degrees, and when there is a tie between columns based on this criterion, the column with the  
 546 larger  $y$  degree is eliminated first.

547 This fitting procedure is continued until no further segments are eliminated. If more than three  
 548 complete cycles that passed the initial editing steps are eliminated in this way, the surface is  
 549 assumed to be too complex for a simple polynomial approximation, and we proceed as follows:

550 (i) the fit and its statistics are reported based on the complete set of pairs that passed  
 551 the initial editing steps (valid pairs), using a planar ( $x$  degree =  $y$  degree = 1) fit in  $x$  and  $y$ .

552 (ii) the *ref\_surf/complex\_surface\_flag* is set to 1.

553 The misfit parameters are reported in the *ref\_surf* group: The final chi-squared statistic is  
 554 reported as *ref\_surf/misfit\_chi2r*, equal to the chi-squared statistic divided by the number of  
 555 degrees of freedom in the solution; the final RMS of the scaled residuals is reported as  
 556 *ref\_surf/misfit\_rms*.

557 **3.3 Reference-shape Correction Error Estimates**

558 We first calculate the errors in the corrected surface heights for segments included in the  
 559 reference-surface fit. We form a second covariance matrix,  $C_1$ , whose diagonal elements are the  
 560 maximum of the squares of the segment errors and  $\langle r^2 \rangle$ . We estimate the covariance matrix for  
 561 the height estimates:

$$C_m = G^{-g} C_1 G^{-gT} \quad 9$$

562 The square roots of the diagonal values of  $C_m$  give the estimated errors in the surface-polynomial  
 563 and height estimates due to short-spatial-scale errors in the segment heights. If there are  $N_{coeff}$   
 564 coefficients in the surface-shape polynomial, and  $N_{shape-cycles}$  cycles included in the surface-shape  
 565 fit, then the first  $N_{coeff}$  diagonal elements of  $C_m$  give the square of the errors in the surface-shape  
 566 polynomial and the last  $N_{shape-cycles}$  give the errors in the surface heights for the cycles included in  
 567 the fit. The portion of  $C_m$  that refers only to the surface shape and surface-shape change  
 568 components is  $C_{m,s}$ .

569 **3.4 Calculating corrected height values for repeats with no selected pairs**

570 Once the surface polynomial has been established from the edited data set, corrected heights are  
 571 calculated for the unselected cycles (*i.e.* those from which all pairs were removed in the editing  
 572 steps): For the segments among these cycles, we form a new surface and slope-change design  
 573 matrix,  $[S, S_t]$  and multiply it by  $[s, s_t]$  to give the surface-shape correction:

$$z_c = z - [S, S_t][s, s_t] \quad 10$$

574 Here  $s$  is the surface-shape polynomial, and  $s_t$  is the slope-change-rate estimate. This gives up to  
 575 fourteen corrected-height values per unselected cycle. From among these, we select the segment  
 576 with the minimum error, as calculated in the next step.

577 The height errors for segments from cycles not included in the surface-shape fit are calculated:

$$\sigma_{z,c}^2 = \text{diag}([S, S_t]C_{m,s}[S, S_t]^T) + \sigma_z^2 \quad 11$$

578 Here  $\sigma_z$  is the error in the segment height, and  $\sigma_{z,c}$  is the error in the corrected height. The  
 579 results of these calculations give a height and a height error for each unselected segment. To  
 580 obtain a corrected elevation for each repeat that contains no selected pairs, we identify the  
 581 segment from that repeat that has the smallest error estimate, and report the value  $z_c$  as that  
 582 repeat's *ptx/h\_corr*, and use  $\sigma_{z,c}$  as its error (*/ptx/h\_corr\_sigma*).

583 **3.5 Calculating systematic error estimates**

584 The errors that have been calculated up to this point are due to errors in fitting segments to  
 585 photon-counting data and due to inaccuracies in the polynomial fitting model. Additional error  
 586 components can result from more systematic errors, such as errors in the position of ICESat-2 as  
 587 derived from POD, and pointing errors from PPD. These are estimated in the ATL06  
 588 *sigma\_geo\_xt*, *sigma\_geo\_at*, and *sigma\_geo\_r* parameters, and their average for each repeat is  
 589 reported in the *cycle\_stats* group under the same parameter names. The geolocation component  
 590 of the total height is the product of the geolocation error and the surface slope, added in  
 591 quadrature with the vertical height error:

$$\sigma_{h,systematic} = \left[ \left( \frac{dh}{dx} \sigma_{geo,AT} \right)^2 + \left( \frac{dh}{dy} \sigma_{geo,XT} \right)^2 + \sigma_{geo,r}^2 \right]^{1/2} \quad 12$$

592 For selected segments, which generally come from pairs containing two high-quality height  
 593 estimates,  $dh/dy$  is estimated from the ATL06  $dh\_fit\_dy$  parameter. For unselected segments, it is  
 594 based on the  $y$  component of the reference-surface slope, as calculated in section 4.2.  
 595 The error for a single segment's corrected height is:

$$\sigma_{h,total} = [\sigma_{h,systematic}^2 + \sigma_{h,c}^2]^{1/2} \quad 13$$

596 This represents the total error in the surface height for a single corrected height. In most cases,  
 597 error estimates for averages of ice-sheet quantities will depend on errors from many segments  
 598 from different reference points, and the spatial scale of the different error components will need  
 599 to be taken into account in error propagation models. To allow users to separate these effects,  
 600 we report both the uncorrelated error,  $/ptx/h\_corr\_sigma$ , and the component due only to  
 601 systematic errors,  $/ptx/h\_corr\_sigma\_systematic$ . The total error is the quadratic sum of the two,  
 602 as described in equation 13.

### 603 3.6 Calculating shape-corrected heights for crossing-track data

604 Locations where groundtracks cross provide opportunities to check the accuracy of  
 605 measurements by comparing surface-height estimates between the groundtracks, and also offers  
 606 the opportunity to generate elevation-change time series that have more temporal detail than the  
 607 91-day repeat cycle can offer for repeat-track measurements.

608 At these crossover points, we use the reference surface calculated in 3.5 to calculate corrected  
 609 elevations for the crossing tracks. We refer to the track for which we have calculated the  
 610 reference surface as the *datum* track, and the other track as the *crossing* track. To calculate  
 611 corrected surface heights for the crossing ICESat-2 orbits, we first select all data from the  
 612 crossing orbit within a distance  $L\_search\_XT$  of the updated reference point on the datum track.  
 613 For most datum reference points, this will yield no crossing data, in which case the calculation  
 614 for that datum point terminates. If crossing data are found, we then calculate the coordinates of  
 615 these points in the reference point's along-track and across-track coordinates. This calculation  
 616 begins by transforming the crossing-track data into local northing and easting coordinates  
 617 relative to the datum reference-point location:

$$\delta N_c = \frac{\pi R_e}{180} (lat_c - lat_d) \quad 14$$

$$\delta E_c = \frac{\pi R_e}{180} (lon_c - lon_d) \cos(lat_c)$$

618 Here  $(lat_d, lon_d)$  are the coordinates of the adjusted datum reference point,  $(lat_c, lon_c)$  are the  
 619 coordinates of the points on the crossing track, and  $R_e$  is the local radius of the WGS84 ellipsoid.  
 620 We then convert the northing and easting coordinates into along-track and across-track  
 621 coordinates based on the azimuth  $\phi$  of the datum track:

$$x_c = \delta N_c \cos(\phi) + \delta E_c \sin(\phi) \quad 15$$

$$y_c = \delta N_c \sin(\phi) - \delta E_c \cos(\phi)$$

622 Using these coordinates, we proceed as we did in 3.4 and 3.5: we generate  $S_k$  and  $S_{kt}$  matrices,  
 623 use them to correct the data and to identify the data point with the smallest error for each

624 crossing cycle. We report the time, error estimate, and corrected height for the minimum-error  
 625 datapoint from each cycle, as well as the location, pair, and track number corresponding to the  
 626 datum point in the */ptx/crossing\_track\_data* group. Because the crossing angles between the  
 627 tracks are oblique at high latitudes, a particular crossing track may appear in a few subsequent  
 628 datum points; in these cases, we expect that the error estimates should vary with the distance  
 629 between the crossing track and the datum track, so that the point with the minimum error should  
 630 correspond to the precise crossing location of the two tracks.

631 To help evaluate the quality of crossing-track data we calculate the *along\_track\_rss* parameter  
 632 for each crossing-track measurement. This parameter gives the RSS of the differences between  
 633 each segment's endpoint heights and the heights of the previous and subsequent segments. A  
 634 segment that is consistent with the previous and next segments in slope and elevation will have a  
 635 small value for this parameter, a segment that is inconsistent (and thus potentially in error) will  
 636 have a large value. Crossing-track measurements that have values greater than 10 m are  
 637 excluded from ATL11 and do not appear in the dataset.

### 638 3.7 Calculating parameter averages

639 ATL11 contains a variety of parameters that mirror parameters in ATL06, but are averaged to the  
 640 140-m ATL11 resolution. Except where noted otherwise, these quantities are weighted averages  
 641 of the corresponding ATL06 values. For selected pairs (i.e. those included in the reference-  
 642 surface fit), the parameters are averaged over the selected segments from each cycle, using  
 643 weights derived from their formal errors, *h\_li\_sigma*. The parameter weighted average for the  $N_k$   
 644 segments from cycle  $k$  is then:

$$\langle q \rangle = \frac{\sum_{i=1}^{N_k} |\sigma_i^{-2}| q_i}{\sum_{i=1}^{N_k} |\sigma_i^{-2}|} \quad 16$$

645 Here  $q_i$  are the parameter values for the segments. For repeats with no selected pairs, recall that  
 646 the corrected height for only one segment is reported in */ptx/h\_corr*; for these, we simply report  
 647 the corresponding parameter values for that selected segment.  
 648

### 649 3.8 Output data editing

650 The output data product includes cycle height estimates only for those cycles that have  
 651 non-systematic error estimates (*/ptx/h\_corr\_sigma*) less than 15 m. All other heights (and their  
 652 errors) are reported as *invalid*.  
 653

654

655 **4.0 LAND ICE PRODUCTS: LAND ICE H (T)(ATL 11/L3B)**

656 Each ATL11 file contains data for a single reference ground track, for one of the subregions  
 657 defined for ATLAS granules (see Figure 6-3). The ATL11 consists of three top-level groups, one  
 658 for each beam pair (*pt1*, *pt2*, *pt3*). Within each pair-track group, there are datasets that give the  
 659 corrected heights for each cycle, their errors, and the reference-point locations. Subgroups  
 660 (*cycle\_stats*, and *ref\_surf*) provide a set of data-quality parameters, and ancillary data describing  
 661 the fitting process, and use the same ordering and coordinates as the top-level group (i.e. any  
 662 dataset within the */ptx/cycle\_stats* and */ptx/ref\_surf* groups refers to the same latitude, longitude,  
 663 and reference points as the corresponding measurements in the */ptx/* groups.) The  
 664 *crossing\_track\_data* group gives height measurements at crossover locations, and has its own set  
 665 of locations and  
 666

667 **4.1.1 File naming convention**

668 ATL11 files are named in the following format:

669 `ATL11_ttttgg_cccc_rrr_vv.h5`

670 Here *tttt* is the rgt number, *gg* is the granule-region number, *cccc* gives the first and last cycles of  
 671 along-track data included in the file (e.g. `_0308_` would indicate that cycles three through eight,  
 672 inclusive, might be included in the along-track solution), and *rrr* is the release number. and *vv* is  
 673 the version number, which is set to one the first time a granule is generated for a given data  
 674 release, and is incremented by one if the granule is regenerated.  
 675

676 **4.2 /ptx group**

677 **4.3**

678 shows the datasets in the *ptx* groups. This group gives the principal output parameters of the  
 679 ATL11. The corrected repeat measurements are in */ptx/h\_corr*, which gives improved height  
 680 measurements based on a surface fit to valid data at paired segments. The associated reference  
 681 coordinates, */ptx/latitude* and */ptx/longitude* give the reference point location, with averaged  
 682 times per repeat, */ptx/delta\_time*. For repeats with no selected pairs, the corrected height is that  
 683 from the selected segment with the lowest error. Two error metrics are given in  
 684 */ptx/h\_corr\_sigma* and */ptx/h\_corr\_sigma\_systematic*. The first gives the error component due to  
 685 ATL06 range errors and due to uncertainty in the reference surface. The second gives the  
 686 component due to geolocation and radial-orbit errors that are correlated at scales larger than one  
 687 reference point; adding these values in quadrature gives the total per-cycle error. Values are only  
 688 reported for */ptx/h\_corr*, */ptx/h\_corr\_sigma*, and */ptx/h\_corr\_sigma\_systematic* for those cycles  
 689 whose uncorrelated errors are less than 15 m; all others are reported as *invalid*. A  
 690 */ptx/quality\_summary* is included for each cycle, based on fit statistics from ATL06.

691

692

Table 4-1 Parameters in the /ptx/ group

Parameter	Units	Dimensions	Description
<i>cycle_number</i>	counts	$I \times N_{cycles}$	Cycle number for each column of the data
<i>latitude</i>	degrees North	$N_{pts} \times I$	Reference point latitude
<i>longitude</i>	degrees East	$N_{pts} \times I$	Reference point longitude
<i>ref_pt</i>	counts	$N_{pts} \times I$	The reference point number, $m$ , counted from the equator crossing of the RGT.
<i>delta_time</i>	seconds	$N_{pts} \times N_{cycles}$	mean GPS time for the segments for each cycle
<i>h_corr</i>	meters	$N_{pts} \times N_{cycles}$	the mean corrected height
<i>h_corr_sigma</i>	meters	$N_{pts} \times N_{cycles}$	the formal error in the corrected height
<i>h_corr_sigma_systematic</i>	meters	$N_{pts} \times N_{cycles}$	the magnitude of the RSS of all errors that might be correlated at scales larger than a single reference point (e.g. pointing errors, GPS errors, etc)
<i>quality_summary</i>	counts	$N_{pts} \times N_{cycles}$	summary flag: zero indicates high-quality cycles: where $\min(\text{signal\_selection\_source}) \leq 1$ and $\min(\text{SNR\_significance}) < 0.02$ , and $\text{ATL06\_summary\_zero\_count} > 0$ .

693

694 **4.4 /ptx/ref\_surf group**

695 Table 4-2 describes the /ptx/ref\_surf group. This group includes parameters describing the  
 696 reference surface fit at each reference point. The polynomial coefficients are given in

697 /ptx/poly\_ref\_surf, sorted first by total degree, then by x-component degree. Because the  
 698 polynomial degree is chosen separately for each reference point, enough columns are provided in  
 699 the /ptx/poly\_ref\_surf and /ptx/poly\_ref\_surf\_sigma to accommodate all possible components up  
 700 to 2<sup>rd</sup> degree in y and 3<sup>th</sup> degree in x, and absent values are filled in with zeros. The  
 701 correspondence between the columns of the polynomial fields and the exponents of the x and y  
 702 terms are given in the /ptx/poly\_exponent\_x and /ptx/poly\_exponent\_y fields. The time origin for  
 703 the slope change is given in the group attribute /ptx/slope\_change\_t0.

**Table 4-2 Parameters in the /ptx/ref\_surf group**

Parameter	Units	Dimensions	Description
dem_h	Meters	$N_{pts} \times 1$	DEM elevation, derived from the ATL06 dem_h parameter
geoid_h	Meters	$N_{pts} \times 1$	geoid elevation, derived from the ATL06 geoid_h parameter
complex_surface_flag	counts	$N_{pts} \times 1$	0 indicates that normal fitting was attempted, 1 indicates that the signal selection algorithm rejected too many repeats, and only a linear fit was attempted
rms_slope_fit	counts	$N_{pts} \times 1$	the RMS of the slope of the fit polynomial within 50 m of the reference point
e_slope	counts	$N_{pts} \times 1$	the mean East-component slope for the reference surface within 50 m of the reference point
n_slope	counts	$N_{pts} \times 1$	the mean North-component slope for the reference surface within 50 m of the reference point
at_slope	Counts	$N_{pts} \times 1$	Mean along-track component of the slope of the reference surface within 50 m of the reference point
xt_slope		$N_{pts} \times 1$	Mean across-track component of the slope of the reference surface within 50 m of the reference point
deg_x	counts	$N_{pts} \times 1$	Maximum degree of non-zero polynomial components in x
deg_y	counts	$N_{pts} \times 1$	Maximum degree of non-zero polynomial components in y
poly_exponent_x	counts	$1 \times 8$	Exponents for the x factors in the surface polynomial
poly_exponent_y	counts	$1 \times 8$	Exponents for the y factors in the surface polynomial
poly_coeffs	counts	$N_{pts} \times 8$	polynomial coefficients (up to degree 3), for polynomial components scaled by 100 m



<i>poly_ref_coeffs_sigma</i>	counts	$N_{pts} \times 8$	formal errors for the polynomial coefficients
<i>ref_pt_number</i>	counts	$N_{pts} \times 1$	Ref point number, counted from the equator crossing along the RGT.
<i>x_atc</i>	meters	$N_{pts} \times 1$	Along-track coordinate of the reference point, measured along the RGT from its first equator crossing.
<i>y_atc</i>	meters	$N_{pts} \times 1$	Across-track coordinate of the reference point, measured along the RGT from its first equator crossing.
<i>rgt_azimuth</i>	degrees	$N_{pts} \times 1$	Reference track azimuth, in degrees east of local north
<i>slope_change_rate_x</i>	years <sup>-1</sup>	$N_{pts} \times 1$	rate of change of the x component of the surface slope
<i>slope_change_rate_y</i>	years <sup>-1</sup>	$N_{pts} \times 1$	rate of change of the y component of the surface slope
<i>slope_change_rate_x_sigma</i>	years <sup>-1</sup>	$N_{pts} \times 1$	Formal error in the rate of change of the x component of the surface slope
<i>slope_change_rate_y_sigma</i>	years <sup>-1</sup>	$N_{pts} \times 1$	Formal error in the rate of change of the y component of the surface slope
<i>misfit_chi2r</i>	meters	$N_{pts} \times 1$	misfit chi square, divided by the number of degrees in the solution
<i>misfit_rms</i>	meters	$N_{pts} \times 1$	RMS misfit for the surface-polynomial fit
<i>fit_quality</i>	counts	$N_{pts} \times 1$	Indicates quality of the fit: 0: no problem identified 1: One or more polynomial coefficient errors larger than 2 2: One or more components of the surface slope has magnitude larger than 0.2 3: Conditions 1 and 2 both true.

704  
705  
706  
707  
708  
709  
710  
711  
712  
713  
714

The slope of the fit surface is given in the *ref\_surf/n\_slope* and *ref\_surf/e\_slope* parameters in the local north and east directions; the corresponding slopes in the along-track and across-track directions are given in the *ref\_surf/xt\_slope* and *ref\_surf/yt\_slope* parameters. For the along-track points, the surface slope is calculated by evaluating the correction-surface polynomial for a 10-m spaced grid of points extending  $\pm 50$  m in x and y around the reference point, and calculating the mean slopes of these points. The calculation is performed in along-track coordinates and then projected onto the local north and east vectors. The *rms\_slope\_fit* is derived from the same set of points, and is calculated as the RMS of the standard deviations of the slopes calculated from adjacent grid points, in x and y.

715

716 **4.5 /ptx/cycle\_stats group**

717 The /ptx/cycle\_stats group gives summary information about the segments present for each  
 718 reference point. Most parameters are averaged according to equation 14, but for others (e.g.  
 719 /ptx/signal\_selection\_flag\_best, which is the minimum of the signal selection flags for the cycle)  
 720 **Table 4-3** describes how the summary statistics are derived.

721

722 **Table 4-3 Parameters in the /ptx/cycle\_stats group**

Parameter	Units	Dimensions	Description
<i>ATL06_summary_zero_count</i>	counts	$N_{pts} \times N_{cycles}$	Number of segments with <i>atl06_quality_summary</i> =0 (0 indicates the best-quality data)
<i>h_rms_misfit</i>	meters	$N_{pts} \times N_{cycles}$	Weighted-average RMS misfit between PE heights and along-track land-ice segment fit
<i>r_eff</i>	counts	$N_{pts} \times N_{cycles}$	Weighted-average effective, uncorrected reflectance for each cycle.
<i>tide_ocean</i>	meters	$N_{pts} \times N_{cycles}$	Weighted-average ocean tide for each cycle
<i>dac</i>	meters	$N_{pts} \times N_{cycles}$	Dynamic atmosphere correction (mainly the effect of atmospheric pressure on floating-ice elevation).
<i>cloud_flg_atm</i>	counts	$N_{pts} \times N_{cycles}$	Minimum cloud flag from ATL06: Flag indicates confidence that clouds with $OT^* > 0.2$ are present in the lower 3 km of the atmosphere based on ATL09
<i>cloud_flg_asr</i>	counts	$N_{pts} \times N_{cycles}$	Minimum apparent-surface-reflectance - based cloud flag from ATL06: Flag indicates confidence that clouds with $OT > 0.2$ are present in the lower 3 km of the atmosphere based on ATL09
<i>bsnow_h</i>	meters	$N_{pts} \times N_{cycles}$	Weighted-average blowing snow layer height for each cycle
<i>bsnow_conf</i>	counts	$N_{pts} \times N_{cycles}$	Maximum <i>bsnow_conf</i> flag from ATL06: indicates the greatest (among

Parameter	Units	Dimensions	Description
			segments) confidence flag for presence of blowing snow for each cycle
<i>x_atc</i>	meters	$N_{pts} \times N_{cycles}$	weighted average of pair-center RGT y coordinates for each cycle
<i>y_atc</i>	meters	$N_{pts} \times N_{cycles}$	weighted mean of pair-center RGT y coordinates for each cycle
<i>ref_pt</i>		$N_{pts} \times N_{cycles}$	Ref point number, counted from the equator crossing along the RGT.
<i>seg_count</i>	counts	$N_{pts} \times N_{cycles}$	Number of segments marked as valid for each cycle. Equal to 0 for those cycles not included in the reference-surface shape fit.
<i>min_signal_selection_source</i>	counts	$N_{pts} \times N_{cycles}$	Minimum of the ATL06 <i>signal_selection_source</i> value (indicates the highest-quality segment in the cycle)
<i>min_snr_significance</i>	counts	$N_{pts} \times N_{cycles}$	Minimum of SNR_significance (indicates the quality of the best segment in the cycle)
<i>sigma_geo_h</i>	meters	$N_{pts} \times N_{cycles}$	Root-mean-weighted-square-average total vertical geolocation error due to PPD and POD
<i>sigma_geo_at</i>	meters	$N_{pts} \times N_{cycles}$	Root-mean-weighted-square-average local-coordinate x horizontal geolocation error for each cycle due to PPD and POD
<i>sigma_geo_xt</i>	meters	$N_{pts} \times N_{cycles}$	Root-mean-weighted-square-average local-coordinate y horizontal geolocation error for each cycle due to PPD and POD
<i>h_mean</i>	meters	$N_{pts} \times N_{cycles}$	Weighted-average of surface heights, not including the correction for the reference surface

723 \*OT (optical thickness) is a measure of signal attenuation used in atmospheric calculations. This  
 724 parameter discussed in ICESat-2 atmospheric products (ATL09)  
 725

726 **4.6 /ptx/crossing\_track\_data group**

727 The /ptx/crossing\_track\_data group (Table 4-4) contains elevation data at crossover locations.  
 728 These are locations where two ICESat-2 pair tracks cross, so data are available from both the  
 729 datum track, for which the granule was generated, and from the crossing track. The data in this  
 730 group represent the elevations and times from the crossing tracks, corrected using the reference  
 731 surface from the datum track. Each set of values gives the data from a single segment on the  
 732 crossing track, that was selected as having the minimum error among all segments on the  
 733 crossing track within the  $2 L\_search\_XT$ –by- $2 L\_search\_AT$  window around the reference point  
 734 on the datum track. The systematic errors are evaluated based on the magnitude of the reference-  
 735 surface slope and the magnitude of the horizontal geolocation error of the crossing-track data.  
 736 Attributes for the group specify the track number and pair-track number of the crossing track.  
 737

**Table 4-4 Parameters in the /ptx/crossing\_track\_data group**

Parameter	Units	Dimensions	Description
<i>ref_pt</i>	counts	$N_{XO} \times 1$	the reference-point number for the datum track
<i>delta_time</i>	years	$N_{XO} \times 1$	time relative to the ICESat-2 reference epoch
<i>h_corr</i>	meters	$N_{XO} \times 1$	WGS-84 height, corrected for the ATL11 surface shape
<i>h_corr_sigma</i>	meters	$N_{XO} \times 1$	error in the height estimate
<i>h_corr_sigma_systematic</i>	meters	$N_{XO} \times 1$	systematic error in the height estimate
<i>ocean_tide</i>	Meters	$N_{XO} \times 1$	Ocean-tide estimate for the crossing track
<i>dac</i>	Meters	$N_{XO} \times 1$	Dynamic atmosphere correction for the crossing track
<i>latitude</i>	degrees	$N_{XO} \times 1$	latitude of the crossover point
<i>longitude</i>	degrees	$N_{XO} \times 1$	longitude of the crossover point
<i>cycle_number</i>	counts	$N_{XO} \times 1$	Cycle number for the crossing data
<i>rgt</i>	counts	$N_{XO} \times 1$	The RGT number for the crossing data
<i>spot_crossing</i>	counts	$N_{XO} \times 1$	The spot number for the crossing data

<i>atl06_quality_summary</i>	counts	$N_{XO} \times I$	quality flag for the crossing data derived from ATL06. 0 indicates no problems detected, 1 indicates potential problems
<i>along_track_rss</i>	meters	$N_{XO} \times I$	Root sum of the squared differences between the heights of the endpoints for the crossing-track segment and the centers of the previous and next segments

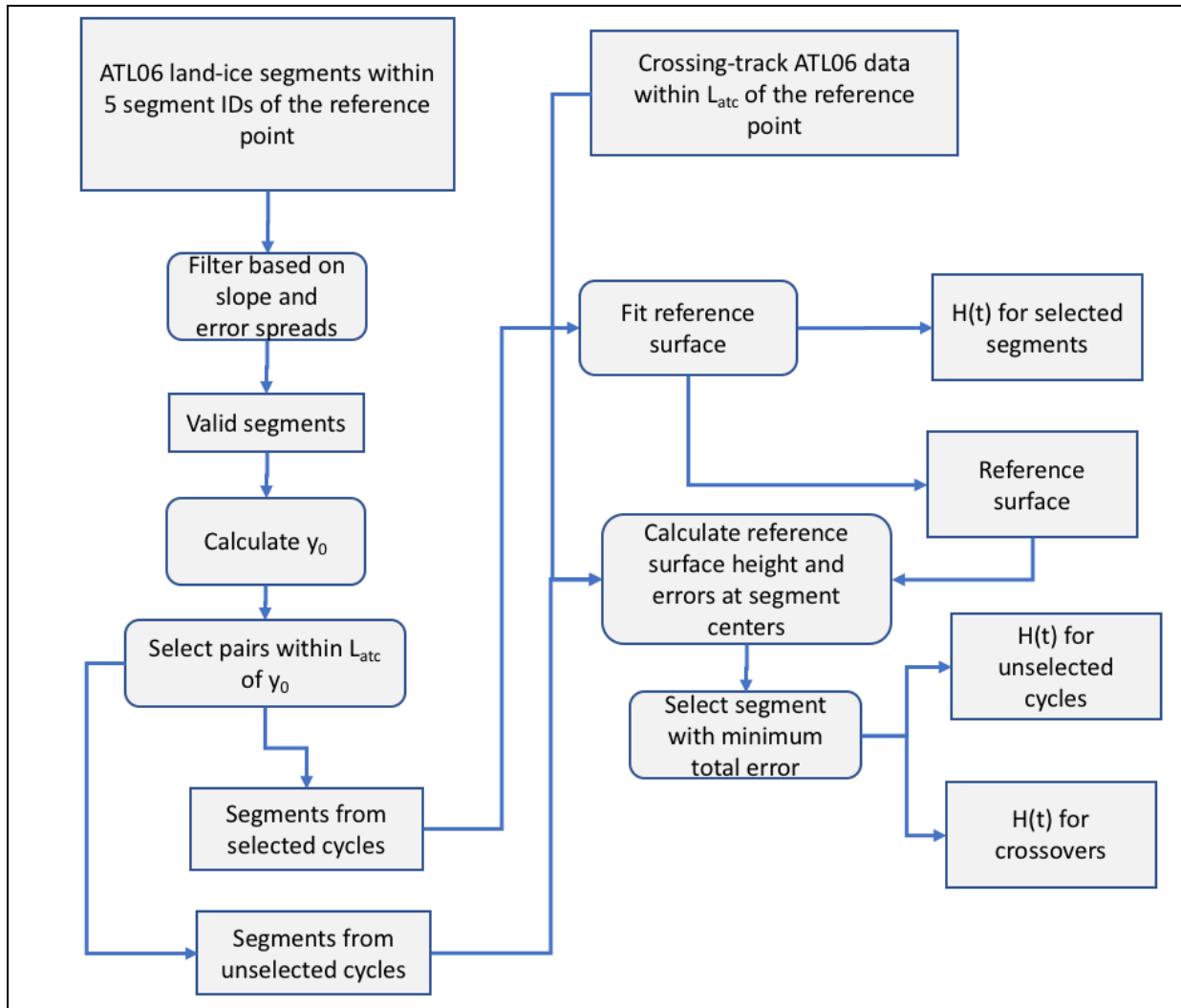
738  
739

740 5.0 ALGORITHM IMPLEMENTATION

741

742

Figure 5-1 Flow Chart for ATL11 Surface-shape Corrections



743

744

745 The following steps are performed for each along-track reference point.

746

747 1. Segments with *segment\_id* within  $N\_search/2$  of the reference-point number, are selected.

748

749 2. Valid segments are identified based on estimated errors, the *ATL06\_quality\_summary* parameter, and the along- and across-track segment slopes. Valid pairs, containing valid measurements from two different beams, are also identified.

750

751 3. The location of the reference point is adjusted to allow the maximum number of repeats with at least one valid pair to fall within the across-track search distance of the reference point.

752

753

- 754 4. The reference surface is fit to pairs with two valid measurements within the search  
 755 distance of the reference point. This calculation also produces corrected heights for the  
 756 selected pairs and the errors in the correction polynomial coefficients.  
 757 5. The correction surface is used to derive corrected heights for segments not selected in  
 758 steps 1-3, and the height for the segment with the smallest error is selected for each  
 759 6. The reference surface is used to calculate heights for external (pre-ICESat-2) laser  
 760 altimetry data sets and crossover ICESat-2 data.  
 761 A schematic of this calculation is shown in Figure 5-1.

### 762 5.1.1 Select ATL06 data for the current reference point

763 **Inputs:**

764 *ref\_pt*: segment number for the current reference point  
 765 *track\_num*: The track number for current point  
 766 *pair\_num*: The pair number for the current point

767 **Outputs:**

768 *D\_ATL06*: ATL06 data structure

769 **Parameters:**

770 *N\_search*: number of segments to search, around *ref\_pt*, equal to 5.

771 **Algorithm:**

- 772 1. For each along-track point, load all ATL06 data from track *track\_num* and pair *pair\_num* that  
 773 have *segment\_id* within *N\_search* of *ref\_pt*: These segments have  $ref\_pt - N\_search$   
 774  $\leq segment\_id \leq ref\_pt + N\_search$ .  
 775 2. Reject any data that have *y\_atc* values more than 500 m distant from the nominal pair-track  
 776 centers (3200 m for pair 1, 0 m for pair 2, -3200 m for pair 3).  
 777

### 778 5.1.2 Select pairs for the reference-surface calculation

779 **Inputs:**

780 *ref\_pt*: reference point number for the current fit  
 781 *x\_atc\_ctr*: Along-track coordinate of the reference point  
 782 *D\_ATL06*: ATL06 data structure  
 783 *pair\_data*: Structure describing ATL06 pairs, includes mean of strong/weak beam *y\_atc* and  
 784 *dh\_fit\_dy*

785 **Outputs:**

786 **validity flags for each segment:**

787 *valid\_segs.x\_slope*: Segments identified as valid based on x-slope consistency  
 788 *valid\_segs.data*: Segments identified as valid based on ATL06 parameter values.

789 **Validity flags for each pair:**

790 *valid\_pairs*: Pairs selected for the reference-surface calculation  
 791 *valid\_pairs.y\_slope*: Pairs identified as valid based on y-slope consistency  
 792 *y\_polyfit\_ctr*: y center of the slope regression  
 793 *ref\_surf/complex\_surface\_flag*: Flag indicating 0: non-complex surface, 1: complex surface.  
 794

795 **Parameters:**

796 *L\_search\_XT*: The across-track search distance.  
 797 *N\_search*: Along-track segment search distance  
 798 *seg\_sigma\_threshold\_min*: Minimum threshold for accepting errors in segment heights, equal to  
 799 0.05 m.

800 **Algorithm:**

801 1. Flag valid segments based on ATL06 values.

802       1a. Count the cycles that contain at least one pair that has *atl06\_quality\_flag*=0  
 803 for both segments. If this number is greater than  $N_{cycles}/3$ , set  
 804 *ref\_surf/complex\_surface\_flag*=0 and set *valid\_segs.data* to 1 for segments with  
 805 *ATL06\_quality\_summary* equal to 0. Otherwise, set *ref\_surf/complex\_surface\_flag*=1 and set  
 806 *valid\_segs.data* to 1 for segments with *snr\_significance* < 0.02.

807       1b. Define *seg\_sigma\_threshold* as the maximum of 0.05 or three times the median of  
 808 *sigma\_h\_li* for segments with *valid\_segs.data* equal to 1. Set *valid\_segs.data* to 1 for segments  
 809 with *h\_sigma\_li* less than this threshold and *ATL06\_quality\_summary* equal to 0.

810       1c. Define *valid\_pairs.data*: For each pair of segments, set *valid\_pairs.data* to 1 when  
 811 both segments are marked as valid in *valid\_segs.data*.

812 2. Calculate representative values for the *x* and *y* coordinate for each pair, and filter by distance.

813       2a. For each pair containing two defined values, set *pair\_data.x* to the segments' *x\_atc*  
 814 value, and *pair\_data.y* to the mean of the segments' *y\_atc* values.

815       2b. Calculate *y\_polyfit\_ctr*, equal to the median of *pair\_data.y* for pairs marked valid in  
 816 *valid\_pairs.data*.

817       2c. Set *valid\_pairs.ysearch* to 1 for pairs with  $|pair\_data.y - y\_polyfit\_ctr| <$   
 818 *L\_search\_XT*.

819 3. Select pairs based on across-track slope consistency

820       3a. Define *pairs\_valid\_for\_y\_fit*, for the across-track slope regression if they are marked  
 821 as valid in *valid\_pairs.data*, and *valid\_pairs.ysearch*, not otherwise.

822       3b. Choose the degree of the regression for across-track slope

823       -If the valid pairs contain at least two different *x\_atc* values (separated by at least  
 824 18 m), set the along-track degree, *my\_regression\_y\_degree*, to 1, 0 otherwise.

825       -If valid pairs contain at least two different *ref\_surf/y\_atc* values (separated by at  
 826 least 18 m), set the across-track degree, *my\_regression\_y\_degree*, to 1, 0 otherwise.

827       3c. Calculate the formal error in the *y* slope estimates: *y\_slope\_sigma* is the RSS of the  
 828 *h\_li\_sigma* values for the two beams in the pair divided by the difference in their *y\_atc*  
 829 values. Based on these, calculate *my\_regression\_tol*, equal to the maximum of 0.01 or three  
 830 times the median of *y\_slope\_sigma* for valid pairs (*pairs\_valid\_for\_y\_fit*).

831       3d. Calculate the regression of *dh\_fit\_dy* against *pair\_data.x* and *pair\_data.y* for valid  
 832 pairs (*pairs\_valid\_for\_y\_fit*). The result is *y\_slope\_model*, which gives the variation of *dh\_fit\_dy*  
 833 as a function of *x\_atc* and *y\_atc*. Calculate *y\_slope\_resid*, the residuals between the *dh\_fit\_dy*  
 834 values and *y\_slope\_model* for all pairs in *pair\_data*.

835       3e. Calculate *y\_slope\_threshold*, equal to the maximum of *my\_regression\_tol* and three  
 836 times the RDE of *y\_slope\_resid* for valid pairs.



837 3f. Mark all pairs with  $|y\_slope\_resid| > y\_slope\_threshold$  as invalid. Re-establish  
 838 *pairs\_valid\_for\_y\_fit* (based on *valid\_pairs.data*, *valid\_pairs.y\_slope* and *valid\_pairs.ysearch*).  
 839 Return to step 3d (allow two iterations total).

840 3g. After the second repetition of 3d-f, use the model to mark all pairs with  
 841  $|y\_slope\_resid|$  less than *y\_slope\_threshold* with 1 in *valid\_pairs.y\_slope*, 0 otherwise.

842 4. Select segments based on along-track slope consistency for both segments in the pair

843 4a. Define *pairs\_valid\_for\_x\_fit*, valid segments for the along-track slope regression:  
 844 segments are valid if they come from pairs marked as valid in *valid\_pairs.data* and  
 845 *valid\_pairs.ysearch*, not otherwise.

846 4b. Choose the degree of the regression for along-track slope

847 -If valid segments contain at least two different *x\_atc* values set the along-track  
 848 degree, *mx\_regression\_x\_degree*, to 1, 0 otherwise.

849 -If valid segments contain at least two different *y\_atc* values, set the across-track  
 850 degree, *mx\_regression\_y\_degree*, to 1, 0 otherwise.

851 4c. Calculate along-track slope regression tolerance, *mx\_regression\_tol*, equal to the  
 852 maximum of either 0.01 or three times the median of the *dh\_fit\_dx\_sigma* values for the valid  
 853 pairs.

854 4d. Calculate the regression of *dh\_fit\_dx* against *pair\_data.x* and *pair\_data.y* for valid  
 855 segments (*pairs\_valid\_for\_x\_fit*). The result is *x\_slope\_model*, which gives the variation of  
 856 *dh\_fit\_dx* as a function of *pair\_data.x* and *pair\_data.y*. Calculate *x\_slope\_resid*, the residuals  
 857 between the *dh\_fit\_dx* and *x\_slope\_resid* for all segments for this reference point, *seg\_x\_center*  
 858 and *y\_polyfit\_ctr*.

859 4e. Calculate *x\_slope\_threshold*, equal to the maximum of either *mx\_regression\_tol* or  
 860 three times the RDE of *x\_slope\_resid* for valid segments.

861 4f. Mark *valid\_segs.x\_slope* with  $|x\_slope\_resid| > x\_slope\_threshold$  as invalid. Re-  
 862 establish *valid\_pairs.x\_slope* when both *valid\_segs.x\_slope* equal 1. Re-establish  
 863 *pairs\_valid\_for\_x\_fit*. Return to step 4d (allow two iterations total).

864 4g. After the second repetition of 4d-f, mark all segments with  $|x\_slope\_resid|$  less than  
 865 *x\_slope\_threshold* with 1 in *seg\_valid\_xslope*, 0 otherwise. Define *valid\_pairs.x\_slope* as 1 for  
 866 pairs that contain two segments with *valid\_segs.x\_slope*=1, 0 otherwise.

867 5. Re-establish *valid\_pairs.all*. Set equal to 1 if *valid\_pairs.x\_slope*, *valid\_pairs.y\_slope*,  
 868 and *valid\_pairs.data* are all valid.

869 5a. Identify *unselected\_cycle\_segs*, as those *D6.cycles* where *valid\_pairs.all* are False.  
 870

### 871 5.1.3 Adjust the reference-point y location to include the maximum number of 872 cycles

#### 873 **Inputs:**

874 *D\_ATL06*: ATL06 structure for the current reference point.

875 *valid\_pairs*: Pairs selected based on parameter values and along- and across-track slopes.

#### 876 **Outputs:**

877 *ref\_surf/y\_atc*: Adjusted fit-point center *y*.

878 *valid\_pairs*: validity masks for pairs, updated to include those identified as valid based on the  
 879 spatial search around *y\_atc\_ctr*.

880 **Parameters:**

881 *L\_search\_XT*: Across-track search length (equal to 110 m)

882 **Algorithm:**

883 1. Define *y0* as the median of the unique integer values of the pair center *y\_atc* for all  
 884 valid pairs. Set a range of *y* values, *y0\_shifts*, as  $\text{round}(y0) \pm 100$  meters in 2-meter increments.

885 2. For each value of *y0\_shifts* (*y0\_shift*), set a counter, *selected\_seg\_cycle\_count*, to the  
 886 number of distinct cycles for which both segments of the pair are contained entirely within the *y*  
 887 interval [*y0\_shift* - *L\_search\_XT*, *y0\_shift* + *L\_search\_XT*]. Add to this, the number of distinct  
 888 cycles represented by unpaired segments contained within that interval, weighted by 0.01. The  
 889 sum is called *score*.

890 3. Search for an optimal *y*-center value (with the most distinct cycles). Set *y\_best* to the  
 891 value of *y0\_shift* that maximizes *score*. If there are multiple *y0\_shift* values with the same,  
 892 maximum *score*, set to the median of the *y0\_shift* values with the maximum *score*.

893 4. Update *valid\_pairs* to include all pairs with *y\_atc* within  $\pm L\_search\_XT$  from  
 894 *y\_atc\_ctr*.

895 **5.1.4 Calculate the reference surface and corrected heights for selected pairs**

896 **Inputs:**

897 *D\_ATL06*: ATL06 structure for the current reference point, containing parameters for each  
 898 segment:

899 *x\_atc*: along-track coordinate

900 *y\_atc*: across-track coordinate

901 *delta\_t*: time for the segment

902 *pair\_data*: Structure containing information about ATL06 pairs. Must include:

903 *y\_atc*: Pair-center across-track coordinates

904 *valid\_pairs*: Pairs selected based on parameter values and along- and across-track slope.

905 *x\_atc\_ctr*: The reference point along-track x coordinate (equal to *ref\_surf/x\_atc*).

906 *y\_atc\_ctr*: The reference point along-track x coordinate (equal to *ref\_surf/y\_atc*)

907 **Outputs:**

908 *ref\_surf/deg\_x*: Degree of the reference-surface polynomial in the along-track direction

909 *ref\_surf/deg\_y*: Degree of the reference-surface polynomial in the across-track direction

910 *ref\_surf/poly\_coeffs*: Polynomial coefficients of the reference-surface fit

911 *ref\_surf/poly\_coeffs\_sigma*: Formal error in polynomial coefficients of the reference-surface fit

912 *ref\_surf/slope\_change\_rate\_x*: Rate of change of the x component of the surface slope

913 *ref\_surf/slope\_change\_rate\_x\_sigma*: Formal error in the rate of change of the x component of  
 914 the surface slope

915 *ref\_surf/slope\_change\_rate\_y*: Rate of change of the y component of the surface slope

916 *ref\_surf/slope\_change\_rate\_y\_sigma*: Formal error in the rate of change of the y component of  
 917 the surface slope

918 *r\_seg*: Segment residuals from the reference-surface model

919 */ptx/h\_corr*: Partially filled-in per-cycle corrected height for cycles used in reference surface

920 */ptx/h\_corr\_sigma*: Partially filled-in per-cycle formal error in corrected height for cycles used in  
 921 reference surface  
 922 *ref\_surf\_cycles*: A list of cycles used in defining the reference surface  
 923 *C\_m\_surf*: Covariance matrix for the reference-polynomial and surface-change model  
 924 *fit\_columns\_surf*: Mask identifying which components of the combined reference-polynomial  
 925 and surface-change model were included in the fit.  
 926 *degree\_list\_x*: The x degrees corresponding to the columns of matrix used in fitting the reference  
 927 surface to the data  
 928 *degree\_list\_y*: The y degrees corresponding to the columns of matrix used in fitting the reference  
 929 surface to the data  
 930 *selected\_segments*: A set of flags indicating which segments were selected by the iterative  
 931 fitting process.  
 932 Partially filled-n per-cycle ATL11 output variables (see table 4-3) for cycles used in reference  
 933 surface  
 934 **Parameters:**  
 935 *poly\_max\_degree\_AT*: Maximum polynomial degree for the along-track fit, equal to 3.  
 936 *poly\_max\_degree\_XT*: Maximum polynomial degree for the across-track fit, equal to 2.  
 937 *slope\_change\_t0*: Half the duration of the mission (equal to the time of the last-possible  
 938 elevation value minus the time of the start of data collection, divided by two).  
 939 *max\_fit\_iterations*: Maximum number of iterations for surface fitting, with acceptable residuals,  
 940 equal to 20.  
 941 *xy\_scale*: The horizontal scaling value used in polynomial fits, equal to 100 m  
 942 *t\_scale*: The time scale used in polynomial fits, equal to seconds in 1 year.  
 943 **Algorithm:**  
 944 1. Build the cycle design matrix: **G<sub>zp</sub>** is a matrix that has one column for each distinct  
 945 cycle in *selected\_pairs* and one row for each segment whose pair is in *selected\_pairs*. For each  
 946 segment, the corresponding row of **G<sub>zp</sub>** is 1 for the column matching the cycle for that segment  
 947 and zero otherwise.  
 948 2. Select the polynomial degree.  
 949 The degree of the x polynomial, *ref\_surf/deg\_x*, is:  
 950  $\min(\text{poly\_max\_degree\_AT}, \text{maximum}(\text{number of distinct values of } \text{round}((x\_atc - x\_atc\_ctr)/20)$   
 951  $\text{among the selected segments in any one cycle}) - 1)$ , and the degree of the y polynomial,  
 952 *ref\_surf/deg\_y*, is :  $\min(\text{poly\_max\_degree\_XT}, \text{number of distinct values of}$   
 953  $\text{round}((\text{pair\_data.y\_atc} - \text{y\_atc\_ctr})/20)$  among the selected pairs)  
 954 3. Perform an iterative fit for the reference-surface polynomial.  
 955 3a. Define *degree\_list\_x* and *degree\_list\_y*: This array defines the x and y degree of the  
 956 polynomial coefficients in the polynomial surface model. There is one component for each  
 957 unique degree combination of x degrees between 0 and *ref\_surf/deg\_x* and for y degree between  
 958 0 and *ref\_surf/deg\_y* such that  $x\_degree + y\_degree \leq \max(\text{ref\_surf/deg\_x}, \text{ref\_surf/deg\_y})$ ,  
 959 except that there is no  $x\_degree=0$  and  $y\_degree=0$  combination. They are sorted first by the  
 960 sum of the x and y degrees, then by x degree, then by y degree.  
 961 3b. Define the polynomial fit matrix. **S<sub>fit\_poly</sub>** has one column for each element of  
 962 the polynomial degree arrays, with values equal to  $((x\_atc - x\_atc\_ctr)/xy\_scale)^{x\_degree} ((y\_atc -$   
 963  $y\_atc\_ctr)/xy\_scale)^{y\_degree}$ . There is one row in the matrix for every segment marked as *selected*.

964 3c. If the time span is longer than 1.5 years, define slope-change matrices,  
 965 **S\_fit\_slope\_change**. The first column of the matrix gives the rate of slope change in the x  
 966 component, equal to  $(x\_atc - x\_atc\_ctr)/xy\_scale*(delta\_time-slope\_change\_t0)/t\_scale$ . The  
 967 second column gives the rate of slope change in the y component, equal to  $(y\_atc -$   
 968  $y\_atc\_ctr)/xy\_scale*(delta\_time-slope\_change\_t0)/t\_scale$ .

969 3d. Build the surface matrix, **G\_surf**, and the combined surface and cycle-height matrix,  
 970 **G\_surf\_zp**: The surface matrix is equal to the horizontal catenation of **S\_fit\_poly**, and, if  
 971 defined, **S\_fit\_slope\_change**. The combined surface and cycle-height matrix, **G\_surf\_zp**, is  
 972 equal to the horizontal catenation of **G\_surf** and **G\_zp**.

973 3e. Subset the fitting matrix. Subset **G\_surf\_zp** by row to include only rows  
 974 corresponding to selected segments to produce **G** (on the first iteration, all are *selected*). Next,  
 975 subset **G** by column, first to eliminate all-zero columns, and second to include only columns that  
 976 are linearly independent from one another: calculate the normalized correlation between each  
 977 pair of columns in **G**, and if the correlation is equal to unity, eliminate the column with the  
 978 higher weighted degree ( $poly\_wt\_sum = x\_degree + 1.1*y\_degree$ , with the factor of 1.1  
 979 chosen to avoid ties). Identify the selected columns in the matrix as *fit\_columns*. If more than  
 980 three of the original surface-change columns have been eliminated, set the  
 981 *ref\_surf/complex\_surface\_flag* to *True*, mark all columns corresponding to polynomial  
 982 coefficients of combined x and y degree greater than 1 as *False* in *fit\_columns*.

983 3f. Check whether the inverse problem is under- or even-determined: If the number of  
 984 *selected\_segments* is less than the number of columns of **G**, eliminate remaining columns of **G** in  
 985 descending order of *poly\_wt\_sum* until the number of columns of **G** is less than the number of  
 986 *selected\_segments*.

987 3g. Generate the data-covariance matrix, **C\_d**. The data-covariance matrix is a square  
 988 matrix whose diagonal elements are the squares of the *h\_li\_sigma* values for the selected  
 989 segments.

990 3h. Calculate the polynomial fit. Initialize **m\_surf\_zp**, the reference model, to a vector of  
 991 zero values, with one value for each column of **G\_surf\_zp**. Calculate the generalized inverse  
 992 (equation 7), of **G**, **G\_g**. If the inversion calculation returns an error, or if any row of **G\_g** is all-  
 993 zero (indicating some parameters are not linearly independent), report fit failure and return.  
 994 Otherwise, multiply **G\_g** by the subset of *h\_li* corresponding to the selected segment to give **m**,  
 995 containing values for the parameters selected in *fit\_columns*. Fill in the components of  
 996 **m\_surf\_zp** flagged in *fit\_columns* with the values in **m**.

997 3i. Calculate model residuals for all segments, *r\_seg*, equal to  $h\_li - G\_surf\_dz *$   
 998 **m\_surf\_zp**. The subset of *r\_seg* corresponding to *selected* segments is *r\_fit*.

999 3j. Calculate the fitting tolerance, *r\_tol*, equal to three times the RDE of the  
 1000  $r\_fit/h\_li\_sigma$  for all *selected* segments. Calculate the reduced chi-squared value for these  
 1001 residuals, *ref\_surf/misfit\_chi2*, equal to  $r\_fit^T C\_d^{-1} r\_fit$ . Calculate the *P* value for the misfit,  
 1002 equal to one minus the CDF of a chi-squared distribution with *m-n* degrees of freedom for  
 1003 *ref\_surf/misfit\_chi2*, where *m* is the number of rows in **G**, and *n* is the number of columns.

1004 3k. If the *P* value is less than 0.025 and fewer than *max\_fit\_iterations* have taken place,  
 1005 mark all segments for which  $|r\_seg/h\_li\_sigma| < r\_tol$  as *selected*, and return to 3e. Otherwise,  
 1006 continue to 3k.

1007 3l. Propagate the errors. Based on the most recent value of  $C\_d$ , generate a revised data-  
 1008 covariance matrix,  $C\_dp$ , whose diagonals values are the maximum of  $h\_li\_sigma^2$  and  
 1009  $RDE(r\_fit)^2$ . Calculate the model covariance matrix,  $C\_m$  using equation 9. If any of the  
 1010 diagonal elements of  $C\_m$  are larger than  $10^4$ , report a fit failure and return. Fill in elements of  
 1011  $m\_surf\_zp$  that are marked as valid in  $fit\_columns$  with the square roots of the corresponding  
 1012 diagonal elements of  $C\_m$ . If any of the errors in the polynomial coefficients are larger than 2,  
 1013 set  $ref\_surf/fit\_quality=1$ .  
 1014 4. Return a list of cycles used in determining the reference surface in  $ref\_surf\_cycles$ . These  
 1015 cycles have columns in  $G$  that contain a valid pair, and for which the steps 3e and 3j did not  
 1016 eliminate the degree of freedom. For these cycles, partially fill in the values of  $/ptx/h\_corr$  and  
 1017  $/ptx/h\_corr\_sigma$ , from  $m$  and  $m\_sigma$ . Similarly, fill in values for  
 1018  $/ptx/h\_corr\_sigma\_systematic$  (Equation 12) and  $/ptx/delta\_time$ , as well as all variables in Table  
 1019 4-3. Set  $/ptx/h\_corr$ ,  $/ptx/h\_corr\_sigma$ ,  $/ptx/h\_corr\_sigma\_systematic$  to  $NaN$  for those cycles  
 1020 that have uncorrelated error estimates greater than 15 m.  
 1021 Values from Table 4-2 defining the fitted reference surface are also reported including  
 1022  $ref\_surf/poly\_coeffs$ , and  $ref\_surf/poly\_coeffs\_sigma$ ,  $ref\_surf/slope\_change\_rate\_x$ ,  
 1023  $ref\_surf/slope\_change\_rate\_y$ ,  $ref\_surf/slope\_change\_rate\_x\_sigma$ , and  
 1024  $ref\_surf/slope\_change\_rate\_y\_sigma$ .  
 1025 Return  $C\_m\_surf$ , the portion of  $C\_m$  corresponding to the polynomial and slope-change  
 1026 components of  $C\_m$ . Return  $selected\_cols\_surf$ , the subset of  $selected\_cols$  corresponding to the  
 1027 surface polynomial and slope-change parameters.  
 1028 Return the reduced chi-square value for the last iteration,  $ref\_surf/misfit\_chi2r$ , equal to  
 1029  $ref\_surf/misfit\_chi2/(m-n)$ .  
 1030

1031 **5.1.5 Calculate corrected heights for cycles with no selected pairs.**

1032 **Inputs:**

1033  $C\_m\_surf$ : Covariance matrix for the reference-surface model.  
 1034  $degree\_list\_x$ ,  $degree\_list\_y$ : List of x-, y-, degrees for which the reference-surface calculation  
 1035 attempted an estimate.  
 1036  $selected\_cols\_surf$ : Parameters of the combined reference-surface and slope-change model for  
 1037 which the inversion returned a value. There should be one value for each row/column of  
 1038  $C\_m\_surf$ .  
 1039  $x\_atc\_ctr$ ,  $y\_atc\_ctr$ : Center point for the surface fit (equal to  $ref\_surf/x\_atc$ ,  $ref\_surf/y\_atc$ )  
 1040  $selected\_segments$ : Boolean array indicating segments selected for the reference-surface  
 1041 calculation  
 1042  $valid\_segs.x\_slope$ : Segments identified as valid based on x-slope consistency  
 1043  $valid\_segs.data$ : Segments identified as valid based on ATL06 parameter values.  
 1044  $pair\_number$ : Pair number for each segment  
 1045  $h\_li$ : Land-ice height for each segment  
 1046  $h\_li\_sigma$ : Formal error in  $h\_li$ .  
 1047  $/ptx/h\_corr$ : Partially filled-in per-cycle corrected height  
 1048  $/ptx/h\_corr\_sigma$ : Partially filled-in per-cycle corrected height error

1049 *ref\_surf/poly\_coeffs*: Polynomial coefficients from 2-d reference-surface fit  
 1050 *ref\_surf\_cycles*: A list of cycles used in defining the reference surface  
 1051 *ref\_surf/slope\_change\_rate\_x*, *ref\_surf/slope\_change\_rate\_y*: Rate of change of the x and y  
 1052 components of the surface slope  
 1053 *ref\_surf/N\_slope*, *ref\_surf/E\_slope*: slope components of reference surface  
 1054 *sigma\_geo\_r*: Radial component of the geolocation error for the crossing track  
 1055 *D\_ATL06*: ATL06 data structure  
 1056 Partially filled-in per-cycle ATL11 output variables (see table 4-3)

1057 **Outputs:**

1058 */ptx/h\_corr*: Per-cycle corrected height  
 1059 */ptx/h\_corr\_sigma*: Per-cycle corrected height error  
 1060 *selected\_segments*: A set of arrays listing the selected segments for each cycle.  
 1061 Per-cycle ATL11 output variables (see table 4-3).

1062 **Algorithm:**

1063 1. Identify the segments marked as valid in *valid\_segs.data* and *valid\_segs.x\_slope* that are not  
 1064 members of the cycles in *ref\_surf\_cycles*. Label these as *non\_ref\_segments*.  
 1065 2. Build **G\_other**, a polynomial-fitting matrix for the *non\_ref\_segments*. **G\_other** will include  
 1066 only the polynomial components listed in *degree\_list\_x* and *degree\_list\_y*, and (if the mission  
 1067 has been going on for at least 1.5 years) the slope-change components. Multiply **G\_other** by  
 1068 [*ref\_surf/poly\_coeffs*, *ref\_surf/slope\_change\_rate\_x*, *ref\_surf/slope\_change\_rate\_y*] to give  
 1069 corrected heights, *z\_kc*.  
 1070 3. Take the subset of **G\_other** corresponding to the components in *fit\_cols\_surf* to make  
 1071 **G\_other\_surf**. Propagate the polynomial surface errors and surface-height errors for  
 1072 *non\_ref\_segments* based on **G\_other\_surf**, **C\_m\_surf**, and *h\_li\_sigma* using equation  
 1073 11. These errors are *z\_kc\_sigma*.  
 1074 4. Identify the segments in *non\_ref\_segments* for each cycle, and, from among these, select the  
 1075 one with the smallest *z\_kc\_sigma*. If, for this cycle, *z\_kc\_sigma* is less than 15 m, fill in the  
 1076 corresponding values of */ptx/h\_corr* and */ptx/h\_corr\_sigma*. For cycles containing no valid  
 1077 segments, report invalid data as NaN. Similarly, fill in the variables in Table 4-3, with the value  
 1078 from the segment with the smallest *z\_kc\_sigma*.

1079

1080 **5.1.6 Calculate corrected heights for crossover data points**

1081 **Inputs:**

1082 *C\_m\_surf*: Covariance matrix for the reference surface model.  
 1083 *C\_m\_surf*: Covariance matrix for the reference-surface model.  
 1084 *x\_atc\_ctr*, *y\_atc\_ctr*: Center point for the surface fit, in along-track coordinates  
 1085 *lat\_d*, *lon\_d*: Latitude and longitude for the adjusted datum reference point (from */ptx/latitude*,  
 1086 */ptx/longitude*)  
 1087 *PT*: Pair track for the surface fit  
 1088 *RGT*: RGT for the surface fit  
 1089 *ref\_surf/rgt\_azimuth*: The azimuth of the RGT, relative to local north  
 1090 *lat\_c*, *lon\_c*: Location for crossover data  
 1091 *time\_c*: Time for crossover data

1092 *h\_c*: Elevations for crossover data  
 1093 *sigma\_h\_c*: Estimated errors for crossover data  
 1094 **Outputs:**  
 1095 *ref\_pt*: reference point (not for the crossing track) (ben, which one then?)  
 1096 *pt*: pair track for the crossing-track points  
 1097 *crossing\_track\_data/rgt*: Reference ground track for the crossing-track point  
 1098 *crossing\_track\_data/delta\_time*: time for the crossing-track point  
 1099 *crossing\_track\_data/h\_corr*: corrected elevation for the crossing-track points  
 1100 *crossing\_track\_data/h\_corr\_sigma*: error in the corrected elevation for the crossing\_track points  
 1101 *crossing\_track\_data/h\_corr\_sigma\_systematic*: Error component in the corrected elevation due  
 1102 to pointing and orbital errors.  
 1103 *crossing\_track\_data/along\_track\_rss*:  
 1104 **Parameters:**  
 1105 *L\_search\_XT*: Across-track search distance  
 1106 **Algorithm (executed independently for the data from each cycle of the mission):**  
 1107 1. Project data points into the along-track coordinate system:  
 1108     1a: Calculate along-track and across-track vectors:  
 1109          $x\_hat = [\cos(\text{ref\_surf}/\text{rgt\_azimuth}), \sin(\text{ref\_surf}/\text{rgt\_azimuth})]$   
 1110          $y\_hat = [\sin(\text{ref\_surf}/\text{rgt\_azimuth}), -\cos(\text{ref\_surf}/\text{rgt\_azimuth})]$   
 1111     1b. Calculate the *R\_earth*, the WGS84 radius at *lat\_d*.  
 1112     1c: Project the crossover data points into a local projection centered on the fit  
 1113 center:  
 1114          $N\_d = R\_earth (\text{lat}_c - \text{lat}_d)$   
 1115          $E\_d = R\_earth \cos(\text{lat}_d) (\text{lon}_c - \text{lon}_d)$   
 1116     1d: Calculate the x and y coordinates for the data points, relative to the fit-center point:  
 1117          $dx\_c = \langle x\_hat, [E\_c, N\_c] \rangle$   
 1118          $dy\_c = \langle y\_hat, [E\_c, N\_c] \rangle$   
 1119     Here  $\langle \mathbf{a}, \mathbf{b} \rangle$  is the inner (dot) product of **a** and **b**.  
 1120 2. Calculate the fitting matrix using equation 6.  
 1121 3. Calculate the errors at each point using the fitting matrix and *C\_m*, using on equation 11.  
 1122 4. Select the minimum-error data point and report the values in Table 4-1.  
 1123 5. Calculate the systematic error in the corrected height:  
 1124      $\text{crossing\_track\_data}/h\_sigma\_sigma\_systematic = (\text{sigma\_geo\_r}^2 + (N\_d$   
 1125  $\text{ref\_surf}/n\_slope)^2 + (E\_d \text{ref\_surf}/e\_slope)^2)^{1/2}$   
 1126 6. Calculate the along-track RSS for the selected segment. For each selected crossing segment  
 1127 calculate the endpoint heights (equal to the segment center height plus or minus 20 meters times  
 1128 the segment's along-track slope), and calculate the RSS of the differences between these heights  
 1129 and the center heights of the previous and subsequent segments. If this RSS difference is greater  
 1130 than 10 m for any cycle, do not report any parameters for that segment's cycle.  
 1131 **5.1.7 Provide error-averaged values for selected ATL06 parameters**  
 1132 **Inputs:**  
 1133 *ATL06 data structure*: ATL06 data to be averaged

1134 *Selected\_segments*: A set of arrays listing the selected segments for each cycle.

1135 *Parameter\_list*: A list of parameters to be averaged

1136 **Outputs:**

1137 *Parameter\_averages*: One value for each parameter and each cycle

1138 **Algorithm:**

1139 1. For each cycle, select the values of *h\_li\_sigma* based on the values within *selected\_segments*.  
 1140 Calculate a set of weights,  $w_i$ , such that the sum of the weights is equal to 1 and each weight is  
 1141 proportional to the inverse square of *h\_li\_sigma*. If only one value is present in  
 1142 *selected\_segments*,  $w_i=1$ .

1143 2. For each parameter, multiply the weights for each cycle by the parameter values, report the  
 1144 averaged value in *parameter\_averages*.

1145 **5.1.8 Provide miscellaneous ATL06 parameters**

1146 **Inputs:**

1147 *ATL06 data structure*: ATL06 data to be averaged

1148 *Selected\_segments*: A set of arrays listing the selected segments for each cycle.

1149 **Outputs:**

1150 Weighted-averaged parameter values, with one value per cycle, filled in with NaN for cycles  
 1151 with no selected segments

1152 *cycle\_stats/h\_robust\_sprd*

1153 *h\_li\_rms\_mean* (ben, I don't see this in the list)

1154 *cycle\_stats/r\_eff*

1155 *cycle\_stats/tide\_ocean*

1156 *cycle\_stats/dac*

1157 *cycle\_stats/bsnow\_h*

1158 *cycle\_stats/x\_atc*

1159 *cycle\_stats/y\_atc*

1160 *cycle\_stats/sigma\_geo\_h*

1161 *cycle\_stats/sigma\_geo\_at*

1162 *cycle\_stats/sigma\_geo\_xt*

1163 *cycle\_stats/h\_mean*

1164 *ref\_surf/dem\_h*

1165 *ref\_surf/geoid\_h*

1166 Parameter minimum values, with one value per cycle, filled in NaN for cycles with no selected  
 1167 segments:

1168 *cycle\_stats/cloud\_flg\_asr*

1169 *cycle\_stats/cloud\_flg\_atm*

1170 *cycle\_stats/bsnow\_conf*

1171 Other parameters:

1172 *cycle\_stats/strong\_spot*: The laser beam number for the strong beam in the pair

1173 **Algorithm:**

1174 1. Select the segments for the cycle indicated in *selected\_segments* from the  
 1175 *ATL06\_data\_structure*.



- 1176 2: Based on *h\_li\_sigma*, calculate the segment weights using equation 14.  
 1177 3.1 For ATL06 parameters *h\_robust\_sprd*, *h\_li\_rms*, *r\_eff*, *tide\_ocean*, *dac*, *bsnow\_h*, *x\_atc*,  
 1178 *y\_atc*, *sigma\_geo\_h*, *sigma\_geo\_at*, *sigma\_geo\_xt*, and *h\_mean* calculate the weighted average  
 1179 of the parameter based on the segment weights. The output parameter names are the same as the  
 1180 input parameter names, in the *cycle\_stats* group.  
 1181 3.2 For ATL06 parameters *dem\_h* and *geoid\_h*, by regression between the measurement  
 1182 location and the reference point location. The output parameter names are the same as the input  
 1183 parameter names, in the *ref\_surf* group.  
 1184 4. For ATL06 parameters *cloud\_flg\_asr* and *cloud\_flg\_atm* report the best (minimum) value  
 1185 from among the selected values. For *bsnow\_conf* report the maximum value from among the  
 1186 selected values.  
 1187 5. For the *cycle\_stats/strong\_spot* attribute, report the laser beam number for the strong beam in  
 1188 the pair.  
 1189

### 1190 5.1.9 Characterize the reference surface

#### 1191 **Inputs:**

- 1192 *poly\_coeffs*: Coefficients of the surface polynomial  
 1193 *rgt\_azimuth*: the azimuth of the reference ground track

#### 1194 **Outputs:**

- 1195 *ref\_surf/n\_slope*: the north component of the reference-surface slope  
 1196 *ref\_surf/e\_slope*: the east component of the reference-surface slope  
 1197 *ref\_surf/at\_slope*: the along-track component of the reference-surface slope  
 1198 *ref\_surf/xt\_slope*: the across-track component of the reference-surface slope  
 1199 *ref\_surf/rms\_slope\_fit*: the rms slope of the reference surface

#### 1200 **Procedure:**

- 1201 1. Calculate the coordinates of a grid of northing and easting offsets around the reference points,  
 1202 each between -50 m and 50 m in 10-meter increments: dN, dE  
 1203 2. Translate the coordinates into along and across-track coordinates:  
 1204  $dx = \cos(\text{rgt\_azimuth}) * dN + \sin(\text{rgt\_azimuth}) * dE$   
 1205  $dy = \sin(\text{rgt\_azimuth}) * dN - \cos(\text{rgt\_azimuth}) * dE$

- 1206 3. Calculate the polynomial surface elevations for the grid points by evaluating the polynomial  
1207 surface at  $dx$  and  $dy$ :  $z\_poly$
- 1208 4. Fit a plane to  $z\_poly$  as a function of  $dN$  and  $dE$ . The North coefficient of the plane is  
1209  $ref\_surf/n\_slope$ , the east component is  $ref\_surf/e\_slope$ , the RMS misfit of the plane is  
1210  $ref\_surf/rms\_slope\_fit$ . If either component of the slope has a magnitude larger than 0.2, add 2 to  
1211  $ref\_surf/fit\_quality$ .
- 1212 5. Fit a plane to  $z\_poly$  as a function of  $dx$  and  $dy$ . The along-track coefficient of the plane is  
1213  $ref\_surf/at\_slope$ , the across-track component is  $ref\_surf/xt\_slope$ .
- 1214

1215 **6.0 APPENDIX A: GLOSSARY**

1216 This appendix defines terms that are used in ATLAS ATBDs, as derived from a document  
1217 circulated to the SDT, written by Tom Neumann. Some naming conventions are borrowed from  
1218 **Spots, Channels and Redundancy Assignments** (ICESat-2-ATSYS-TN-0910) by P. Luers.  
1219 Some conventions are different than those used by the ATLAS team for the purposes of making  
1220 the data processing and interpretation simpler.

1221  
1222 **Spots.** The ATLAS instrument creates six spots on the ground, three that are weak and three that  
1223 are strong, where strong is defined as approximately four times brighter than weak. These  
1224 designations apply to both the laser-illuminated spots and the instrument fields of view. The  
1225 spots are numbered as shown in Figure 1. At times, the weak spots are leading (when the  
1226 direction of travel is in the ATLAS +x direction) and at times the strong spots are leading.  
1227 However, the spot number does not change based on the orientation of ATLAS. The spots are  
1228 always numbered with 1L on the far left and 3R on the far right of the pattern. Not: beams,  
1229 footprints.

1230  
1231 **Laser pulse (pulse for short).** Individual pulses of light emitted from the ATLAS laser are  
1232 called laser pulses. As the pulse passes through the ATLAS transmit optics, this single pulse is  
1233 split into 6 individual transmit pulses by the diffractive optical element. The 6 pulses travel to  
1234 the earth's surface (assuming ATLAS is pointed to the earth's surface). Some attributes of a laser  
1235 pulse are the wavelength, pulse shape and duration. Not: transmit pulse, laser shot, laser fire.

1236  
1237 **Laser Beam.** The sequential laser pulses emitted from the ATLAS instrument that illuminate  
1238 spots on the earth's surface are called laser beams. ATLAS generates 6 laser beams. The laser  
1239 beam numbering convention follows the ATLAS instrument convention with strong beams  
1240 numbered 1, 3, and 5 and weak beams numbered 2, 4, and 6 as shown in the figures. Not:  
1241 beamlet.

1242  
1243 **Transmit Pulse.** Individual pulses of light emitted from the ICESat-2 observatory are called  
1244 transmit pulses. The ATLAS instrument generates 6 transmit pulses of light from a single laser  
1245 pulse. The transmit pulses generate 6 spots where the laser light illuminates the surface of the  
1246 earth. Some attributes of a given transmit pulse are the wavelength, the shape, and the energy.  
1247 Some attributes of the 6 transmit pulses may be different. Not: laser fire, shot, laser shot, laser  
1248 pulse.

1249  
1250 **Reflected Pulse.** Individual transmit pulses reflected off the surface of the earth and viewed by  
1251 the ATLAS telescope are called reflected pulses. For a given transmit pulse, there may or may  
1252 not be a reflected pulse. Not: received pulse, returned pulse.

1253  
1254 **Photon Event.** Some of the energy in a reflected pulse passes through the ATLAS receiver  
1255 optics and electronics. ATLAS detects and time tags some fraction of the photons that make up  
1256 the reflected pulse, as well as background photons due to sunlight or instrument noise. Any

1257 photon that is time tagged by the ATLAS instrument is called a photon event, regardless of  
1258 source. Not: received photon, detected photon.

1259  
1260 **Reference Ground Track (RGT).** The reference ground track (RGT) is the track on the earth at  
1261 which a specified unit vector within the observatory is pointed. Under nominal operating  
1262 conditions, there will be no data collected along the RGT, as the RGT is spanned by GT2L and  
1263 GT2R (which are not shown in the figures, but are similar to the GTs that are shown). During  
1264 spacecraft slews or off pointing, it is possible that ground tracks may intersect the RGT. The  
1265 precise unit vector has not yet been defined. The ICESat-2 mission has 1387 RGTs, numbered  
1266 from 0001xx to 1387xx. The last two digits refer to the cycle number. Not: ground tracks, paths,  
1267 sub-satellite track.

1268  
1269 **Cycle Number.** Over 91 days, each of the 1387 RGTs will be targeted in the Polar Regions  
1270 once. In subsequent 91-day periods, these RGTs will be targeted again. The cycle number  
1271 tracks the number of 91-day periods that have elapsed since the ICESat-2 observatory entered the  
1272 science orbit. The first 91-day cycle is numbered 01; the second 91-day cycle is 02, and so on.  
1273 At the end of the first 3 years of operations, we expect the cycle number to be 12. The cycle  
1274 number will be carried in the mid-latitudes, though the same RGTs will (in general) not be  
1275 targeted more than once.

1276  
1277 **Sub-satellite Track (SST).** The sub-satellite track (SST) is the time-ordered series of latitude  
1278 and longitude points at the geodetic nadir of the ICESat-2 observatory. In order to protect the  
1279 ATLAS detectors from damage due to specular returns, and the natural variation of the position  
1280 of the observatory with respect to the RGT throughout the orbit, the SST is generally not the  
1281 same as the RGT. Not: reference ground track, ground track.

1282  
1283 **Ground Tracks (GT).** As ICESat-2 orbits the earths, sequential transmit pulses illuminate six  
1284 ground tracks on the surface of the earth. The track width is approximately 10m wide. Each  
1285 ground track is numbered, according to the laser spot number that generates a given ground  
1286 track. Ground tracks are therefore always numbered with 1L on the far left of the spot pattern  
1287 and 3R on the far right of the spot pattern. Not: tracks, paths, reference ground tracks, footpaths.

1288  
1289 **Reference Pair Track (RPT).** The reference pair track is the imaginary line halfway between  
1290 the planned locations of the strong and weak ground tracks that make up a pair. There are three  
1291 RPTs: RPT1 is spanned by GT1L and GT1R, RPT2 is spanned by GT2L and GT2R (and may be  
1292 coincident with the RGT at times), and RPT3 is spanned by GT3L and GT3R. Note that this is  
1293 the planned location of the midway point between GTs. We will not know this location very  
1294 precisely prior to launch. Not: tracks, paths, reference ground tracks, footpaths, pair tracks.

1295  
1296 **Pair Track (PT).** The pair track is the imaginary line half way between the actual locations of  
1297 the strong and weak ground tracks that make up a pair. There are three PTs: PT1 is spanned by  
1298 GT1L and GT1R, PT2 is spanned by GT2L and GT2R (and may be coincident with the RGT at  
1299 times), and PT3 is spanned by GT3L and GT3R. Note that this is the actual location of the

1300 midway point between GTs, and will be defined by the actual location of the GTs. Not: tracks,  
1301 paths, reference ground tracks, footpaths, reference pair tracks.  
1302

1303 **Pairs.** When considered together, individual strong and weak ground tracks form a pair. For  
1304 example, GT2L and GT2R form the central pair of the array. The pairs are numbered 1 through  
1305 3: Pair 1 is comprised of GT1L and GT1R, pair 2 is comprised of GT2L and GT2R, and pair 3 is  
1306 comprised of GT3L and 3R.  
1307

1308 **Along-track.** The direction of travel of the ICESat-2 observatory in the orbit frame is defined as  
1309 the along-track coordinate, and is denoted as the +x direction. The positive x direction is  
1310 therefore along the Earth-Centered Earth-Fixed velocity vector of the observatory. Each pair has  
1311 a unique coordinate system, with the +x direction aligned with the Reference Pair Tracks.  
1312

1313 **Across-track.** The across-track coordinate is y and is positive to the left, with the origins at the  
1314 Reference Pair Tracks.  
1315

1316 **Segment.** An along-track span (or aggregation) of PE data from a single ground track or other  
1317 defined track is called a segment. A segment can be measured as a time duration (e.g. from the  
1318 time of the first PE to the time of the last PE), as a distance (e.g. the distance between the  
1319 location of the first and last PEs), or as an accumulation of a desired number of photons.  
1320 Segments can be as short or as long as desired.  
1321

1322 **Signal Photon.** Any photon event that an algorithm determines to be part of the reflected pulse.  
1323

1324 **Background Photon.** Any photon event that is not classified as a signal photon is classified as a  
1325 background photon. Background photons could be due to noise in the ATLAS instrument (e.g.  
1326 stray light, or detector dark counts), sunlight, or mis-classified signal photons. Not: noise  
1327 photon.  
1328

1329 **h\_\*\*.** Signal photons will be used by higher-level products to determine height above the  
1330 WGS-84 reference ellipsoid, using a semi-major axis (equatorial radius) of 6378137m and a  
1331 flattening of 1/298.257223563. This can be abbreviated as ‘ellipsoidal height’ or ‘height above  
1332 ellipsoid’. These heights are denoted by h; the subscript \*\* will refer to the specific algorithm  
1333 used to determine that elevation (e.g. is = ice sheet algorithm, si = sea ice algorithm, etc...). Not:  
1334 elevation.  
1335

1336 **Photon Cloud.** The collection of all telemetered photon time tags in a given segment is the (or  
1337 a) photon cloud. Not: point cloud.  
1338

1339 **Background Count Rate.** The number of background photons in a given time span is the  
1340 background count rate. Therefore a value of the background count rate requires a segment of PEs  
1341 and an algorithm to distinguish signal and background photons. Not: Noise rate, background  
1342 rate.  
1343

1344 **Noise Count Rate.** The rate at which the ATLAS instrument receives photons in the absence of  
1345 any light entering the ATLAS telescope or receiver optics. The noise count rate includes PEs  
1346 due to detector dark counts or stray light from within the instrument. Not: noise rate,  
1347 background rate, and background count rate.

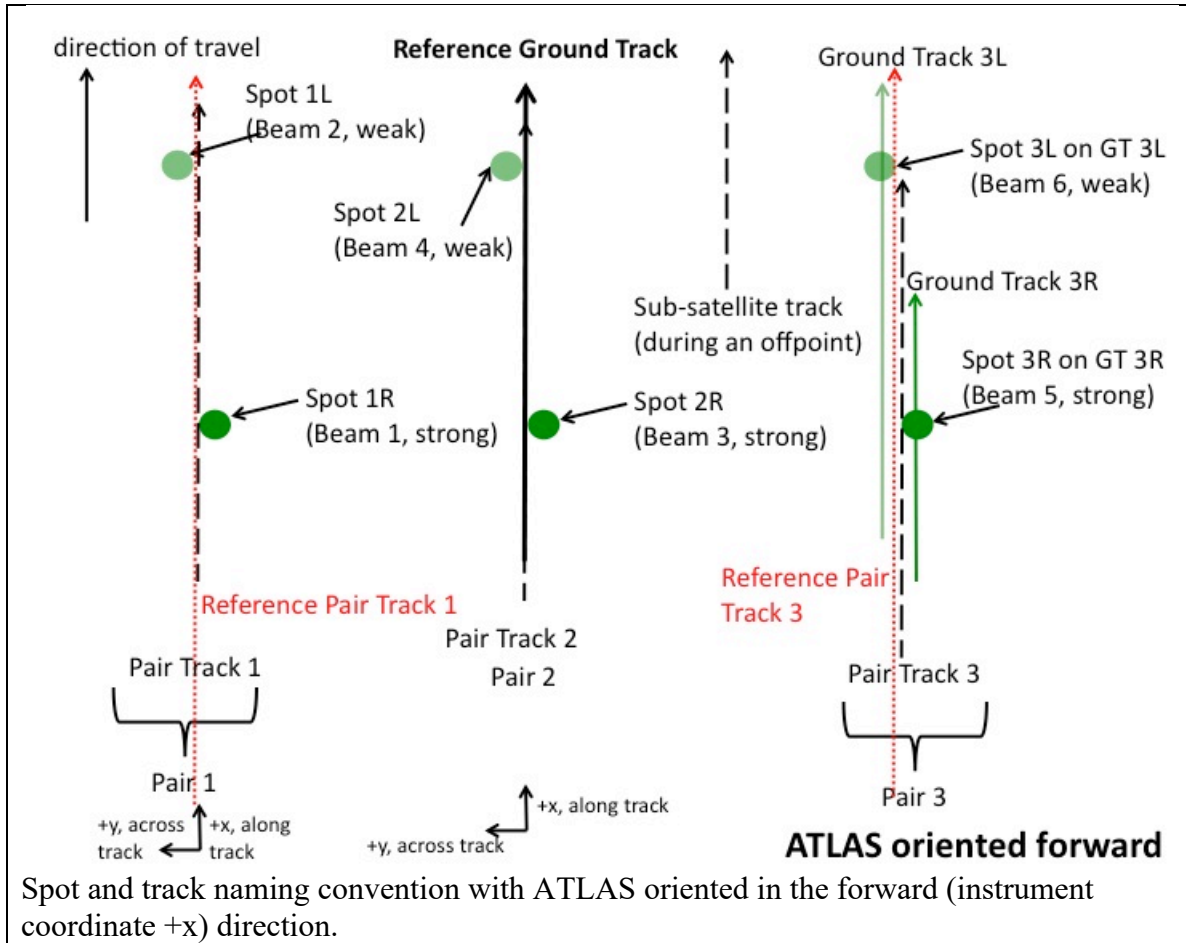
1348  
1349 **Telemetry band.** The subset of PEs selected by the science algorithm on board ATLAS to be  
1350 telemetered to the ground is called the telemetry band. The width of the telemetry band is a  
1351 function of the signal to noise ratio of the data (calculated by the science algorithm onboard  
1352 ATLAS), the location on the earth (e.g. ocean, land, sea ice, etc...), and the roughness of the  
1353 terrain, among other parameters. The widths of telemetry bands are adjustable on-orbit. The  
1354 telemetry bandwidth is described in Section 7 or the ATLAS Flight Science Receiver Algorithms  
1355 document. The total volume of telemetered photon events must meet the data volume constraint  
1356 (currently 577 GBits/day).

1357  
1358 **Window, Window Width, Window Duration.** A subset of the telemetry band of PEs is called a  
1359 window. If the vertical extent of a window is defined in terms of distance, the window is said to  
1360 have a width. If the vertical extent of a window is defined in terms of time, the window is said to  
1361 have a duration. The window width is always less than or equal to the telemetry band.

1362  
1363  
1364  
1365  
1366

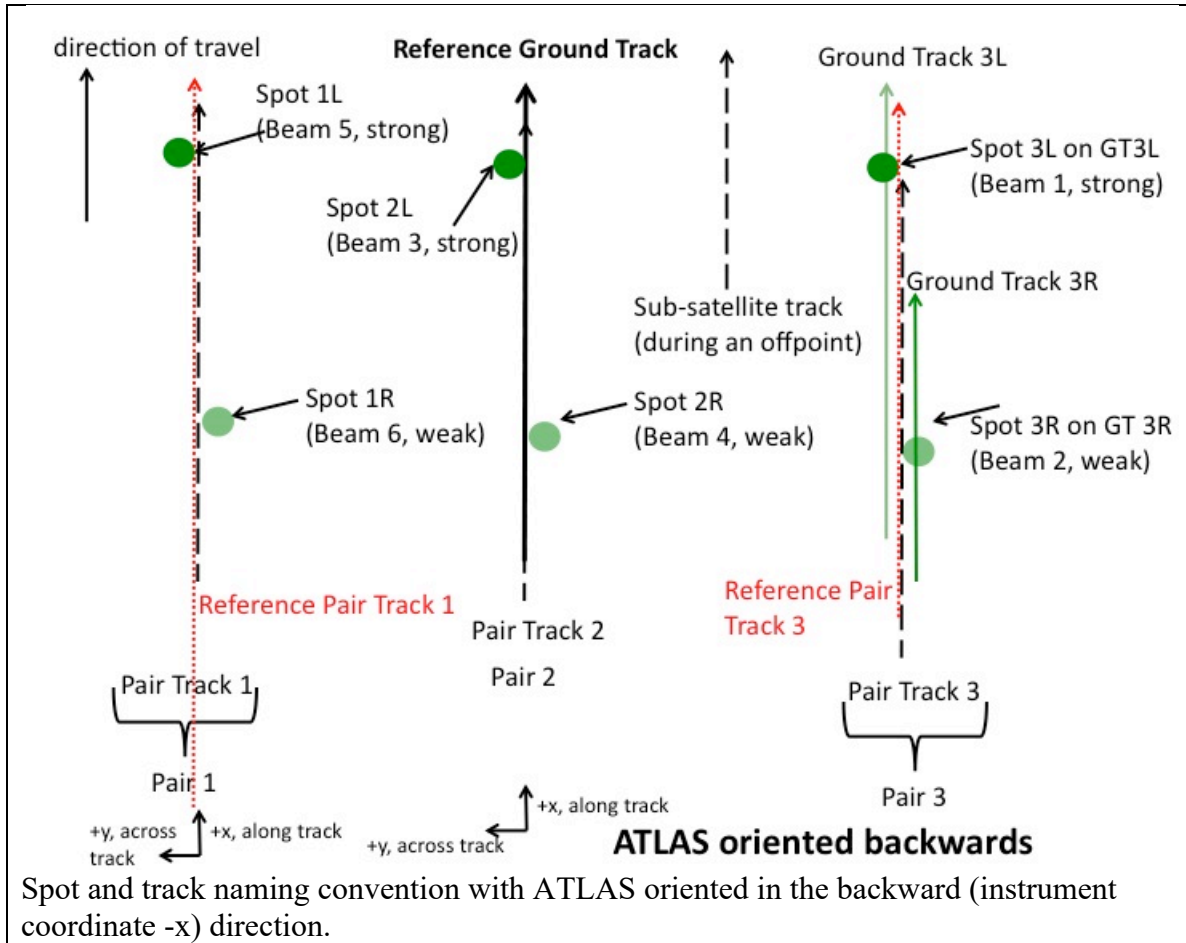
---

Figure 6-1. Spots and tracks, forward flight



1367  
 1368  
 1369  
 1370  
 1371  
 1372  
 1373  
 1374  
 1375  
 1376

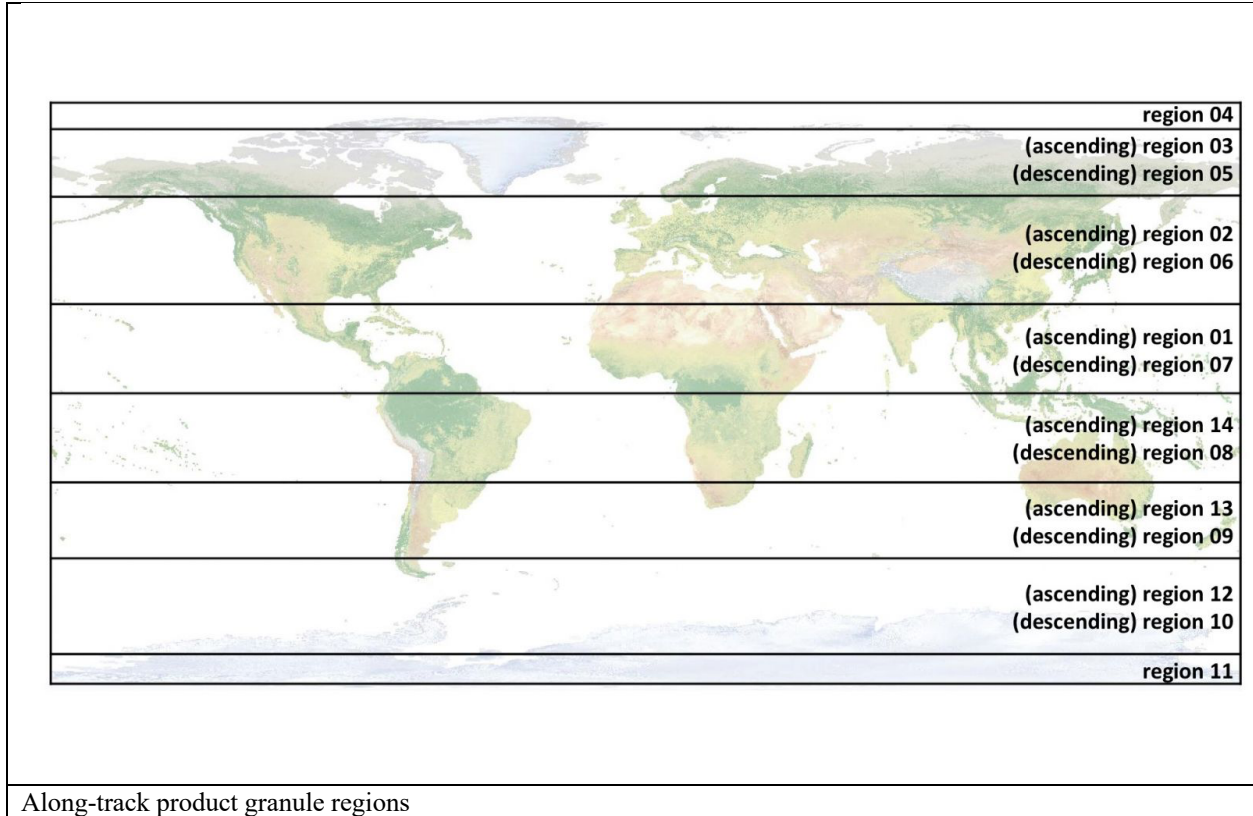
Figure 6-2. Spots and tracks, backward flight



1377

Figure 6-3. Granule regions





1378 **7.0 BROWSE PRODUCTS**

1379 For each ATL11 data file, there will be eight figures written to an associated browse file. Two of  
 1380 these figures are required and are located in the default group; default1 and default2. The browse  
 1381 filename has the same pattern as the data filename, namely,  
 1382 ATL11\_tttss\_c1c2\_rr\_vVVV\_BRW.h5, where tttt is the reference ground track, ss is the orbital  
 1383 segment, c1 is the first cycle of data in the file, c2 is the last cycle of data in the file, rr is the  
 1384 release and VVV is the version. Optionally, the figures can also be written to a pdf file.

1385  
 1386 Below is a discussion of the how the figures are made, with examples from the data file  
 1387 ATL11\_009403\_0307\_02\_vU07.h5. Note that the figure numbering in this section is distinct  
 1388 from that in the rest of the document; the figures shown here are labeled as they are in each  
 1389 browse-product file.

1390  
 1391  
 1392

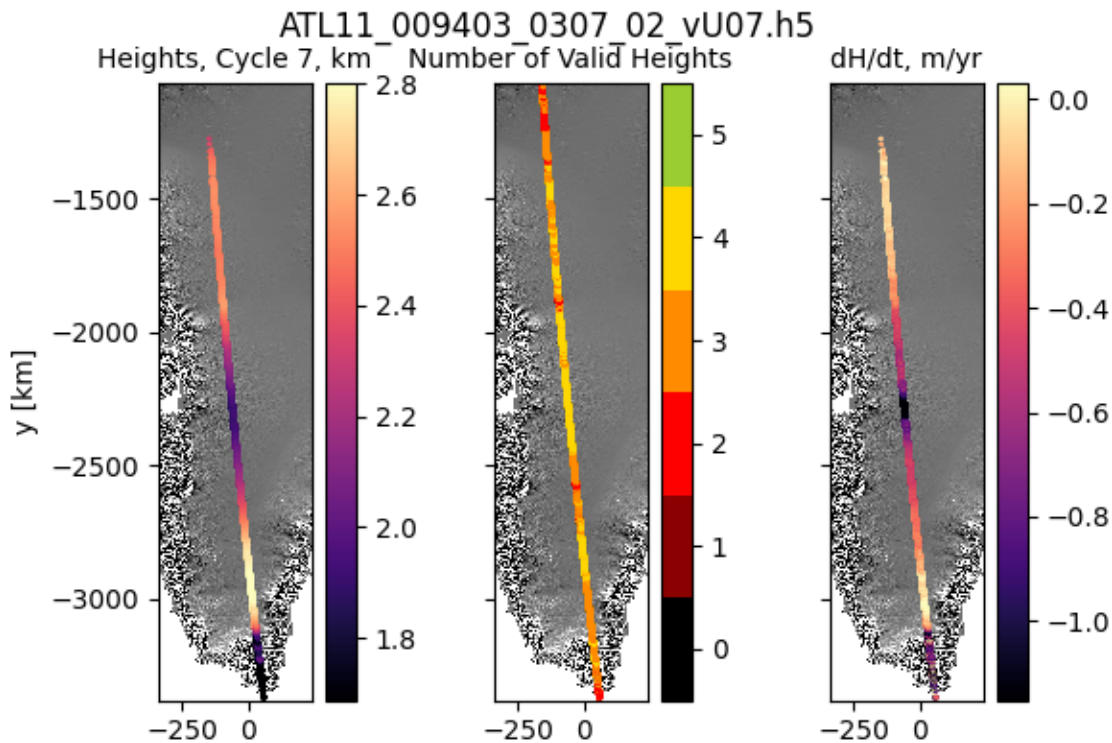


Figure 1. Height data, in km, from cycle 7 (1st panel). Number of cycles with valid height data (2nd panel). Change in height over time, in meters/year, cycle 7 from cycle 3 (3rd panel). All overlaid on gradient of DEM. x, y in km. Maps are plotted in a polar-stereographic projection with a central longitude of 45W and a standard latitude of 70N.

1393  
 1394  
 1395  
 1396

The background for the three panels in Figure 1 is the gradient DEM in gray scale. It is shown in a polar-stereographic projection with a central longitude of 45W (0E) and a standard latitude of

1397 70N (71S), for the Northern (Southern) Hemisphere. The map is bounded by the extent of height  
 1398 data plus a buffer. ATL11 heights (/ptx/h\_corr) from all pairs of the latest cycle with valid data,  
 1399 here cycle 7, are plotted in the first panel. The “magma” color map indicates the heights in km.  
 1400 The limits on the color bar are set with the python scipy.stat.scoreatpercentile method at 5% and  
 1401 95%. In the second panel are plotted the number of valid heights summed over all cycles at each  
 1402 location. The color bar extends to the total number of cycles in the data file. The change in height  
 1403 over time, dH/dt, is plotted in the third panel, in meters/year. dHdt is the change in height of the  
 1404 last cycle with valid data from the first cycle with valid data (/ptx/h\_corr) divided by the  
 1405 associated times (/ptx/delta\_time). Text of ‘No Data’ is printed in the panel if there is only one  
 1406 cycle with valid data, or if the first and last cycles with valid data have no common reference  
 1407 point numbers (/ptx/ref\_pt). All plots are in x,y coordinates, in km. This figure is called  
 1408 default/default1 in the BRW.h5 file.  
 1409

ATL11\_009403\_0307\_02\_vU07.h5

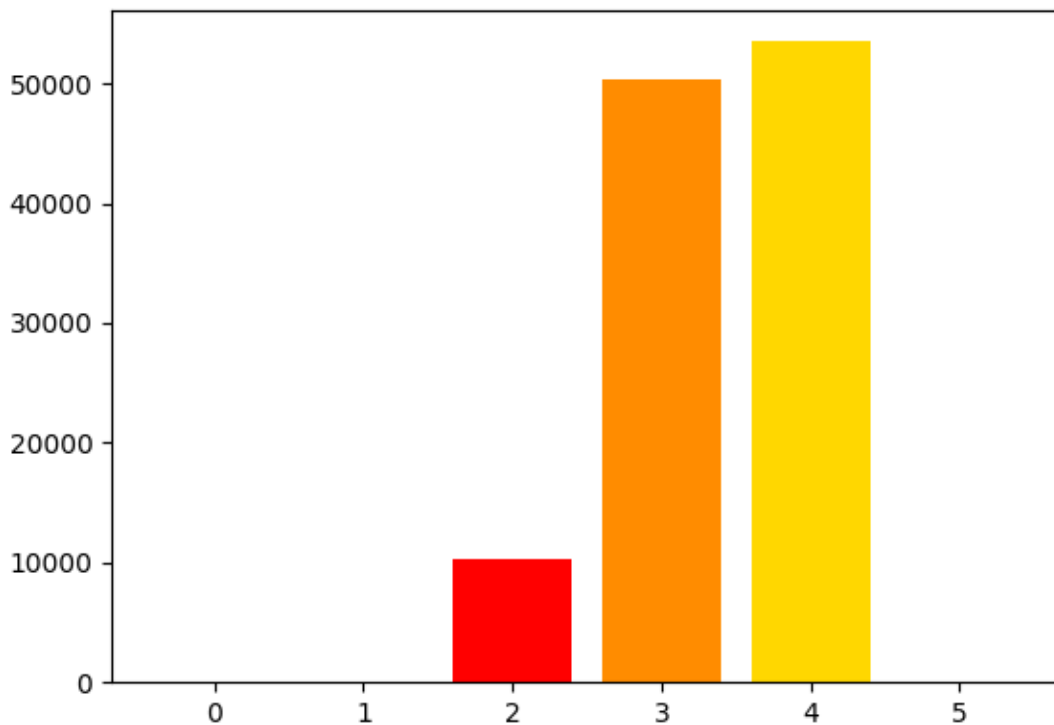


Figure 2. Histogram of number of cycles with valid height measurements, all beam pairs.

1410  
 1411 A histogram of the number of valid height measurements (/ptx/h\_corr) is in Figure 2. Valid  
 1412 height data are summed across all cycles, for each reference point number (/ptx/ref\_pt). The  
 1413 color scale is from zero to the total number of cycles in the data file and matches those in Figure  
 1414 1, 2<sup>nd</sup> panel. This figure is called validrepeats\_hist in the BRW.h5 file.  
 1415  
 1416

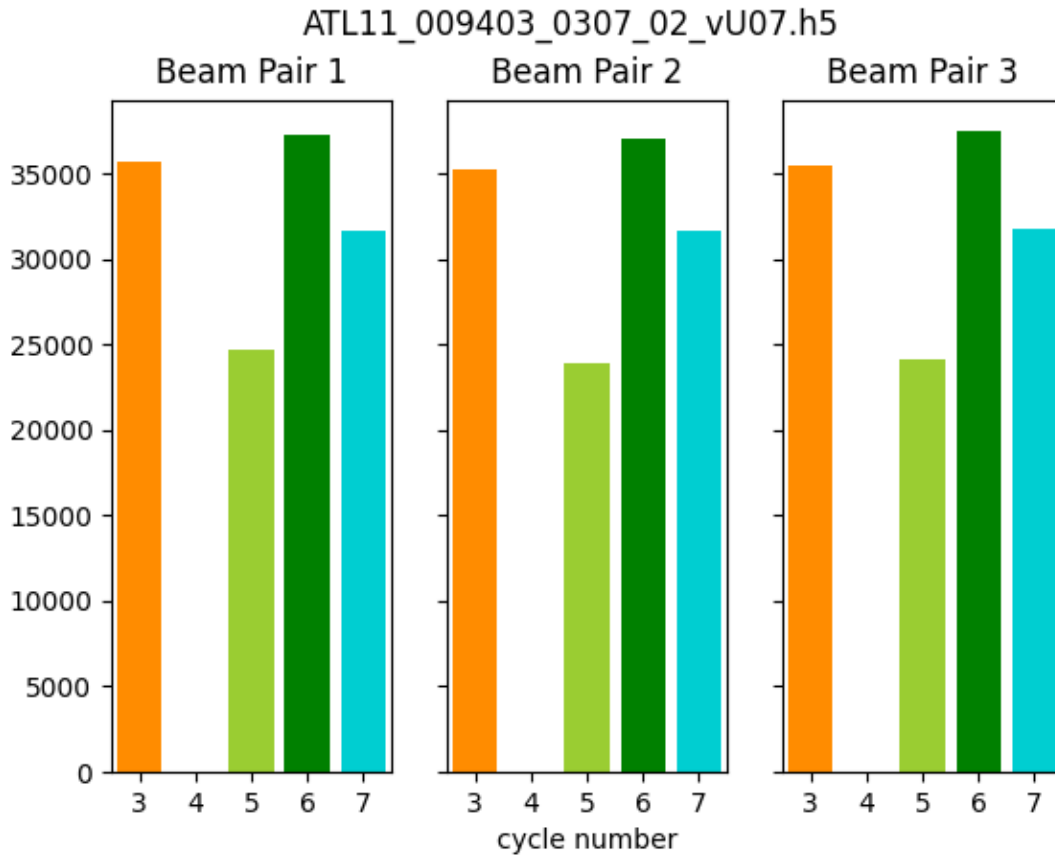


Figure 3. Number of valid height measurements from each beam pair.

1417  
 1418  
 1419  
 1420  
 1421  
 1422

Histograms in Figure 3 show the number of valid heights (/ptx/h\_corr) for each cycle, separated by beam pair. The cycle numbers are color coded. This figure is called default/default2 in the BRW.h5 file.

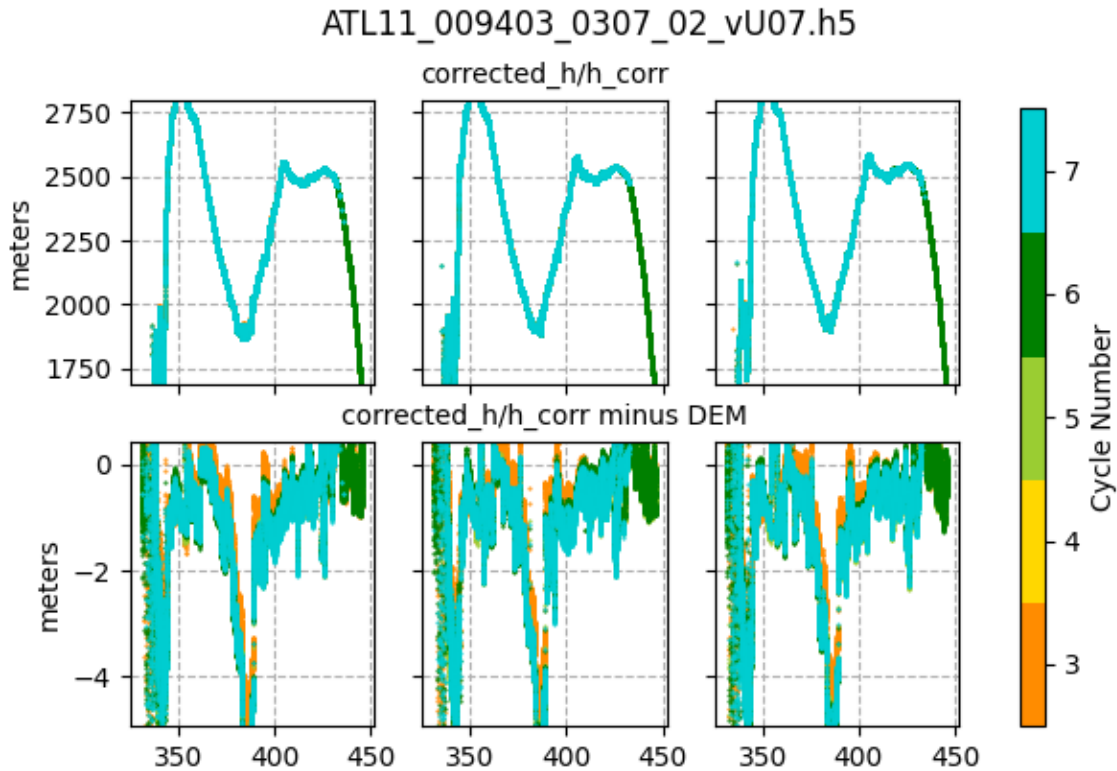


Figure 4. Top row: Heights, in meters, plotted for each beam pair: 1 (left), 2 (center), 3 (right). Bottom row: Heights minus DEM, in meters. Y-axis limits are scores at 5% and 95%. Color coded by cycle number. Plotted against reference point number/1000.

1423  
 1424  
 1425  
 1426  
 1427  
 1428  
 1429  
 1430  
 1431  
 1432  
 1433  
 1434

There are six panels in Figure 4, with two rows and three columns. In the top row are plotted the height measurements ( $/ptx/h\_corr$ ) for each beam pair, one pair per panel. In the bottom row are plotted the same height measurements minus the collocated DEM ( $ref\_surf/dem\_h$ ) values, one pair per panel. The plots are color coded by cycle number, as in Figure 3. The heights are plotted versus reference point number ( $/ptx/ref\_pt$ ) divided by 1000 for a cleaner plot. The y-axis is in meters for both rows. The y-axis limits for the top and bottom rows are set separately, using the `python scipy.stats.scoreatpercentile` method with limits of 5% and 95% for heights and height differences, respectively. Text of 'No Data' is printed in a panel if there are no valid height data for that pair. This figure is called `h_corr_h_corr-DEM` in the `BRW.h5` file.

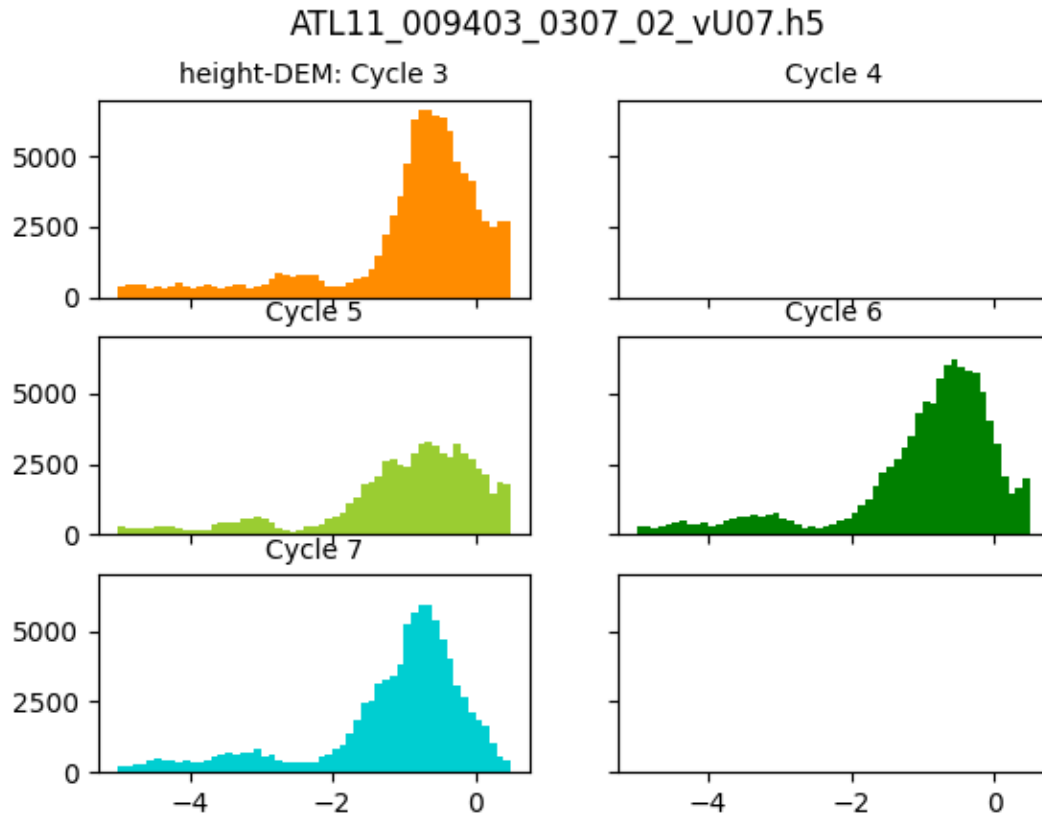


Figure 5. Histograms of heights minus DEM heights, in meters. One histogram per cycle, all beam pairs. X-axis limits are the scores at 5% and 95%.

1435  
1436  
1437  
1438  
1439  
1440  
1441  
1442  
1443

Figure 5 is associated with Figure 4. It is a multi-paneled figure, with the number of panels dependent on the number of cycles in the data file. Each panel is a histogram of the heights (/ptx/h\_corr) minus collocated DEM heights (ref\_surf/dem\_h) color coded by cycle, the same as in Figures 3 and 4. The limits on the histograms are set using the python `scipy.stats.scoreatpercentile` method with limits of 5 and 95% for all cycles of data, the same values used in Figure 4 bottom row. This figure is called `h_corr-DEM_hist` in the BRW.h5 file.

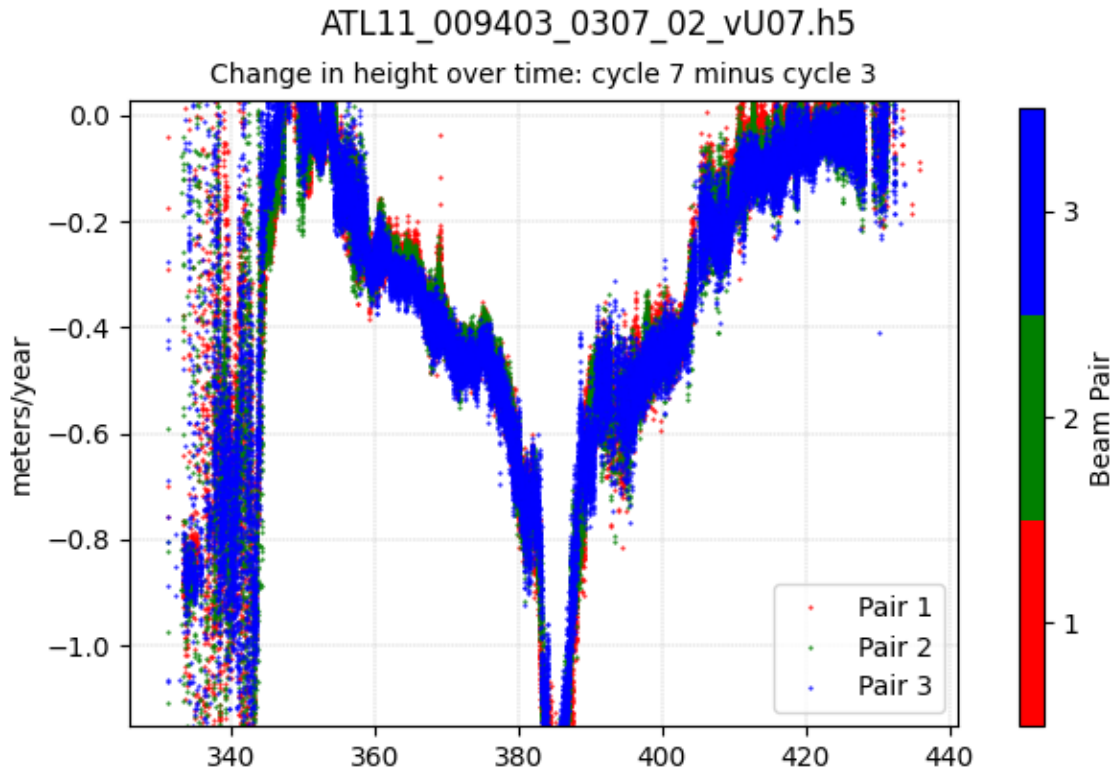


Figure 6. Change in height over time,  $dH/dt$ , in meters/year.  $dH/dt$  is cycle 7 from cycle 3. Color coded by beam pair: 1 (red), 2 (green), 3 (blue). Y-axis limits are scores at 5% and 95%. Plotted against reference point number/1000.

1444  
1445  
1446  
1447  
1448  
1449  
1450  
1451  
1452  
1453  
1454  
1455

The changes in height with time,  $dH/dt$ , in meters/year are plotted in Figure 6. The calculation differences the first and last cycles with valid height data ( $/ptx/h\_corr$ ) divided by the associated time differences ( $/ptx/delta\_time$ ). The change in heights for pair 1 are in red, for pair 2 are in green and for pair 3 are in blue. The y-axis limits are set using the python `scipy.stats.scoreatpercentile` method with limits of 5% and 95%. The x-axis is reference point number ( $/ptx/ref\_pt$ ) divided by 1000 for a cleaner plot. Text of 'No Data' is printed in the panel if there is only one cycle with valid data, or if the first and last cycles with valid data have no common reference point numbers. This figure is called `dHdt` in the `BRW.h5` file.

1456

**Glossary/Acronyms**

ASAS	ATLAS Science Algorithm Software
ATBD	Algorithm Theoretical Basis Document
ATLAS	ATLAS Advance Topographic Laser Altimeter System
CDF	Cumulative Distribution Function
DEM	Digital Elevation Model
GSFC	Goddard Space Flight Center
GTs	Ground Tracks
ICESat-2	Ice, Cloud, and Land Elevation Satellite-2
IKR	I Know, Right?
MABEL	Multiple altimeter Beam Experimental Lidar
MIS	Management Information System
NASA	National Aeronautics and Space Administration
PE	Photon Event
POD	Precision Orbit Determination
PPD	Precision Pointing Determination
PRD	Precise Range Determination
PSO	ICESat-2 Project Science Office
PTs	Pair Tracks
RDE	Robust Dispersion Estimate
RGT	Reference Ground Track
RMS	Root Mean Square
RPTs	Reference Pair Tracks
RT	Real Time
SCoRe	Signature Controlled Request
SIPS	ICESat-2 Science Investigator-led Processing System
TLDR	Too Long, Didn't Read
TBD	To Be Determined



1457

**References**

1458 Brunt, K.M., H.A. Fricker and L. Padman 2011. Analysis of ice plains of the Filchner-Ronne Ice  
1459 Shelf, Antarctica, using ICESat laser altimetry. *Journal of Glaciology*, **57**(205): 965-975.

1460 Fricker, H.A., T. Scambos, R. Bindshadler and L. Padman 2007. An active subglacial water  
1461 system in West Antarctica mapped from space. *Science*, **315**(5818): 1544-1548.

1462 Schenk, T. and B. Csatho 2012. A New Methodology for Detecting Ice Sheet Surface Elevation  
1463 Changes From Laser Altimetry Data. *Ieee Transactions on Geoscience and Remote Sensing*,  
1464 **50**(9): 3302-3316.

1465 Smith, B., H.A. Fricker, N. Holschuh, A.S. Gardner, S. Adusumilli, K.M. Brunt, B. Csatho, K.  
1466 Harbeck, A. Huth, T. Neumann, J. Nilsson and M.R. Siegfried 2019a. Land ice height-retrieval  
1467 algorithm for NASA's ICESat-2 photon-counting laser altimeter. *Remote Sensing of*  
1468 *Environment*: 111352.

1469 Smith, B.E., H.A. Fricker, I.R. Joughin and S. Tulaczyk 2009. An inventory of active subglacial  
1470 lakes in Antarctica detected by ICESat (2003-2008). *Journal of Glaciology*, **55**(192): 573-595.

1471 Smith, B.E., D. Hancock, K. Harbeck, L. Roberts, T. Neumann, K. Brunt, H. Fricker, A.  
1472 Gardner, M. Siegfried, S. Adusumilli, B. Csatho, N. Holschuh, J. Nilsson and F. Paolo 2019b.  
1473 Algorithm Theoretical Basis Document for Land-Ice Along-track Product (ATL06). Goddard  
1474 Space Flight Center.

1475